CH-54A DESIGN AND OPERATIONAL FLIGHT LOADS STUDY

A. L. Mongillo, Jr., et al

United Aircraft Corporation

Prepared for:

Army Air Mobility Research and Development Laboratory

November 1973

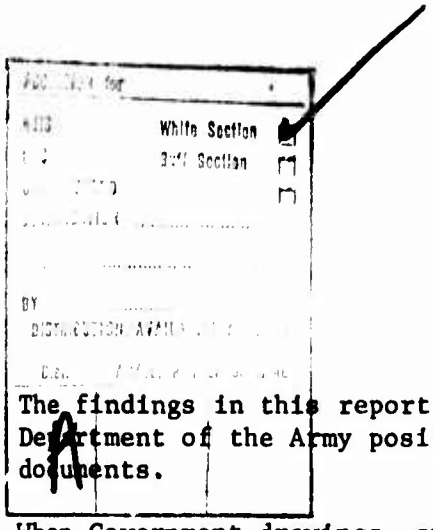

DISCLAIMERS

The findings in this report are not to be construed as an official Department of the Army position unless so designated by other authorized documents.

When Government drawings, specifications, or other data are used for any purpose other than in connection with a definitely related Government procurement operation, the United States Government thereby incurs no responsibility nor any obligation whatsoever; and the fact that the Government may have formulated, furnished, or in any way supplied the said drawings, specifications, or other data is not to be regarded by implication or otherwise as in any manner licensing the holder or any other person or corporation, or conveying any rights or permission, to manufacture, use, or sell any patented invention that may in any way be related thereto.

Trade names cited in this report do not constitute an official endorsement or approval of the use of such commercial hardware or software.

DISPOSITION INSTRUCTIONS

Destroy this report when no longer needed. Do not return it to the originator.

UNCLASSIFIED
Security Classification

AD-77355 /

DOCUMENT CONTROL DATA - R & D

(Security classification of title, body of abstract and indexing annotation must be entered when the overall report is classified)

1. ORIGINATING ACTIVITY *(Corporate author)* Sikorsky Aircraft Division United Aircraft Corporation Stratford, Connecticut	2a. REPORT SECURITY CLASSIFICATION Unclassified 2b. GROUP

3. REPORT TITLE

CH-54A DESIGN AND OPERATIONAL FLIGHT LOADS STUDY

4. DESCRIPTIVE NOTES *(Type of report and inclusive dates)*

Final Report

5. AUTHOR(S) *(First name, middle initial, last name)*

A. L. Mongillo, Jr.
S. M. Johnson

6. REPORT DATE	7a. TOTAL NO. OF PAGES	7b. NO. OF REFS
November 1973	~~75~~ 79	13

8a. CONTRACT OR GRANT NO.	9a. ORIGINATOR'S REPORT NUMBER(S)
DAAJ02-72-C-0060 mw b. PROJECT NO. c. Task 1F162204AA8201 d.	USAAMRDL Technical Report 73-39 9b. OTHER REPORT NO(S) *(Any other numbers that may be assigned this report)* SER-64370

10. DISTRIBUTION STATEMENT

Approved for public release; distribution unlimited.

11. SUPPLEMENTARY NOTES	12. SPONSORING MILITARY ACTIVITY
	Eustis Directorate, U. S. Army Air Mobility Research and Development Laboratory, Fort Eustis, Virginia

13. ABSTRACT

An analytical and correlation study of predicted fatigue design data and operational flight loads data for crane-type helicopters was conducted to compare operational mission profiles with a design mission profile and to provide data for use in establishing structural design criteria for future Army helicopters.

Flight loads and usage data for CH-54A helicopters operating in Southeast Asia were compared with CH-54A design data. The effects of gross weight and altitude on true airspeed were determined. Fatigue spectra were developed for six dynamic components, and fatigue lives were calculated for these components. These fatigue lives were compared with lives predicted during CH-54A design. Service histories for these components were reviewed, and it was found that none of the changes made in these components resulted from load conditions. Peak operational load parameters were compared with limit static design values. Recommendations were then developed to assist in establishing future crane helicopter fatigue design criteria.

DD FORM 1 NOV 1473 REPLACES DD FORM 1473, 1 JAN 64, WHICH IS OBSOLETE FOR ARMY USE.

UNCLASSIFIED
Security Classification

14. KEY WORDS	LINK A		LINK B		LINK C	
	ROLE	WT	ROLE	WT	ROLE	WT
CH-54A Helicopter Flight Spectra Helicopter Operations Aircraft Structures						

DEPARTMENT OF THE ARMY
U.S ARMY AIR MOBILITY RESEARCH & DEVELOPMENT LABORATORY
EUSTIS DIRECTORATE
FORT EUSTIS, VIRGINIA 23604

This program was conducted under Contract DAAJ02-72-C-0060 with Sikorsky Aircraft Division, United Aircraft Corporation.

The information presented herein is the result of an analytical effort to derive improved structural design criteria for crane-type helicopters based upon flight parameters measured on crane helicopters operating in Southeast Asia. This is one of four similar efforts being conducted concurrently to develop improved criteria for observation, gunship, and transport as well as crane-type helicopters.

The report has been reviewed by the Eustis Directorate, U.S. Army Air Mobility Research and Development Laboratory and is considered to be technically sound. It is published for the exchange of information and the stimulation of future research.

This program was conducted under the technical management of Mr. Herman I. MacDonald, Jr., Technology Applications Division.

Task 1F162204AA8201
Contract DAAJ02-72-C-0060
USAAMRDL Technical Report 73-39
November 1973

CH-54A DESIGN AND OPERATIONAL FLIGHT LOADS STUDY

Final Report

Sikorsky Aircraft Report SER-64370

By

A. L. Mongillo, Jr.
S. M. Johnson

Prepared By

Sikorsky Aircraft Division
United Aircraft Corporation
Stratford, Connecticut

for

EUSTIS DIRECTORATE
U. S. ARMY AIR MOBILITY RESEARCH AND DEVELOPMENT LABORATORY
FORT EUSTIS, VIRGINIA

ABSTRACT

Sikorsky Aircraft has conducted an analysis and correlation study of predicted fatigue design data and operational flight loads data for crane-type helicopters. The purpose of the study was to compare operational mission profiles with a design mission profile and to provide data for use in establishing structural design criteria for future Army helicopters.

In this study, flight loads and usage data from USAAVLABS Technical Report 70-73, "Flight Loads Investigation of CH-54A Helicopters Operating in Southeast Asia," were compared with CH-54A design data. The effects of gross weight and altitude on true airspeed were determined. Fatigue spectra were developed for six dynamic components, and fatigue lives were calculated for these components. These fatigue lives were compared with lives predicted during CH-54A design. Service histories for these components were reviewed, and it was found that none of the changes made in these components resulted from load conditions. Peak operational load parameters were compared with limit static design values. Recommendations were then developed to assist in establishing future crane helicopter fatigue design criteria.

Comparison of CH-54A operational mission profiles with the design mission profile indicated that crane operating conditions in a combat environment were generally less severe than predicted. The fatigue substantiation of the six selected components confirmed this. Extended or "unlimited" replacement times resulted for all six components.

Airspeeds above 90 knots were rarely associated with an external payload configuration. Most aircraft flight time occurred in a density altitude range of 2000 to 5000 feet. Approximately 97% of the measured load factor peaks occurred at gross weights at or below 29,000 pounds.

Future Army helicopter designs will benefit from improved data collection and editing techniques. Better definition of discrete ground and flight regimes is required to develop accurate mission profiles. Consideration should be given to development of a composite operational spectrum based upon a combat environment and on peace-time operation. Knowledge of peak loads and specific load parameters, such as main rotor head moment or main and tail rotor flapping angles, would yield more accurate fatigue load prediction.

FOREWORD

This report covers the work performed by Sikorsky Aircraft to analyze and correlate CH-54A design and operational fatigue spectrums. The program was authorized by the U.S. Army Air Mobility Research and Development Laboratory, Fort Eustis, Virginia, under Contract DAAJ02-72-C-0060, Task 1F162204AA8201. The project monitor for the Army was Mr. H. I. MacDonald, Jr.

The authors express appreciation to Messrs. M. Chrissanthis, G. Chuga, A. Clarke, R. Frye, W. Jackson, E. McLaud, and L. Vacca of Sikorsky Aircraft for their contributions to this report.

TABLE OF CONTENTS

LIST OF ILLUSTRATIONS

LIST OF TABLES

SYMBOLS

$C_{T/\sigma}$	Nondimensional blade loading
D	Fatigue damage per 100 hours for entire mission profile
d_i	Fatigue damage per 100 hours for a particular segment of the mission profile
F_G	Bending stress on main rotor shaft at strain gage location, psi
H_1, H_2, H_3, H_4	Time ratio for distribution of altitude in each mission segment, t_{hi}/t
h_d	Density altitude, ft
KIAS	Indicated airspeed, kn
L	Distance from centerline of hub to strain gage location on main rotor shaft, in.
M_B	Bending moment on main rotor shaft at strain gage location due to blade flapping, in.-lb
M_G	Net bending moment on main rotor shaft at strain gage location, in.-lb
M_H	Bending moment at centerline of main rotor hub, in.-lb
M_S	Tail rotor spindle moment, in.-lb
n	Number of segments in the mission profile contributing to fatigue damage
N_Z	Vertical load factor at aircraft center of gravity, g
P_V	Main rotor vibratory pushrod load, lb
R_A	Time ratio for ascent portion of each mission segment, t_A/T
R_C	Time ratio for cruise portion of each mission segment, $(t_C - t_{HOV})/T$
R_D	Time ratio for descent portion of each mission segment, t_D/T
S/N	Curve indicating cycles to crack detection

T	Total time for a particular data sample, min
t	Time for each mission segment, min
TAS	True airspeed, kn
T_A	Total ascent time, percent
T_C	Total cruise time, percent
T_D	Total descent time, percent
t_A	Time in each mission segment for climb rates $\geq$ +300 ft/min, min
t_C	Time in each mission segment for climb rates $\geq$ -300 ft/min but < +300 ft/min, min
t_D	Time in each mission segment for climb rates < -300 ft/min, min
t_{hi}	Time in each mission segment for a particular altitude group, min
t_{HOV}	Time in each mission segment for μ <0.05 at climb rates $\geq$ -300 ft/min but < +300 ft/min, min
T_{MR}	Main rotor axial thrust, lb
t_{vi}	Time in each mission segment for a particular speed group, min
t_{wi}	Time in each mission segment for a particular gross weight group, min
V_{DL}	Limit dive speed, KTAS
V_H	Limit operating speed, KTAS
V_1, V_2, V_3, V_4, V_5	Time ratio for distribution of airspeed in each mission segment, t_{vi}/t
W_1, W_2, W_3	Time ratio for distribution of gross weight in each mission segment, t_{wi}/t
Z	Main rotor shaft section modulus at strain gage location, $in.^3$
β	Main rotor flapping angle, deg

μ	Advance ratio, $\frac{V}{\Omega R}$
ρ	Air density, slug/ft^3
ρ_o	Air density, sea level standard, slug/ft^3
ϕ	Aircraft bank angle, deg
ΩR	Rotor tip speed, ft/sec

INTRODUCTION

The CH-54A crane helicopter was used extensively in Southeast Asia to assist in U.S. Army airmobile operations. During regular missions, several CH-54As were instrumented to record flight data for an operational flight loads report. The resulting report, USAAVLABS Technical Report 70-73, "Flight Loads Investigation of CH-54A Helicopters Operating in Southeast Asia" (Reference 1), was used in the present study to establish a rational approach for development of future crane helicopters and to improve fatigue criteria for dynamic component design. Figure 1 shows a three-view drawing, basic data, and design limits for the CH-54A.

In the present study, fatigue spectra are developed for six components: the main rotor pitch control horn, main rotor shaft, main rotor hub, tail rotor spindle, magnesium main rotor spacer, and aluminum main rotor spacer. The main rotor pitch control horn analysis employs a spectrum of main rotor vibratory pushrod loads, and the tail rotor spindle fatigue analysis employs a spectrum of tail rotor spindle moments. The main rotor shaft, hub, and spacer fatigue analyses employ a spectrum of main rotor head hub moments. Fatigue lives are then compared with current replacement times to assess the impact of the operational flight loads spectrum on life-limited components.

A historical summary tracing changes in component fatigue lives or configurations is presented to identify any situation in which the need for design improvement was indicated.

Comparison of reported maximum one-time occurrences of selected load parameters with structural limit design values indicates that service usage of the CH-54A was predominantly within the structural design limits of the aircraft. However, in certain instances the aircraft were operated above the design gross weight and the design speed. A rational basis is proposed for predicting the frequency of occurrence of maneuver and gust load factors for future crane helicopters.

Finally, recommendations are made to facilitate the derivation of future mission profiles, and conclusions are offered based on the results of this study.

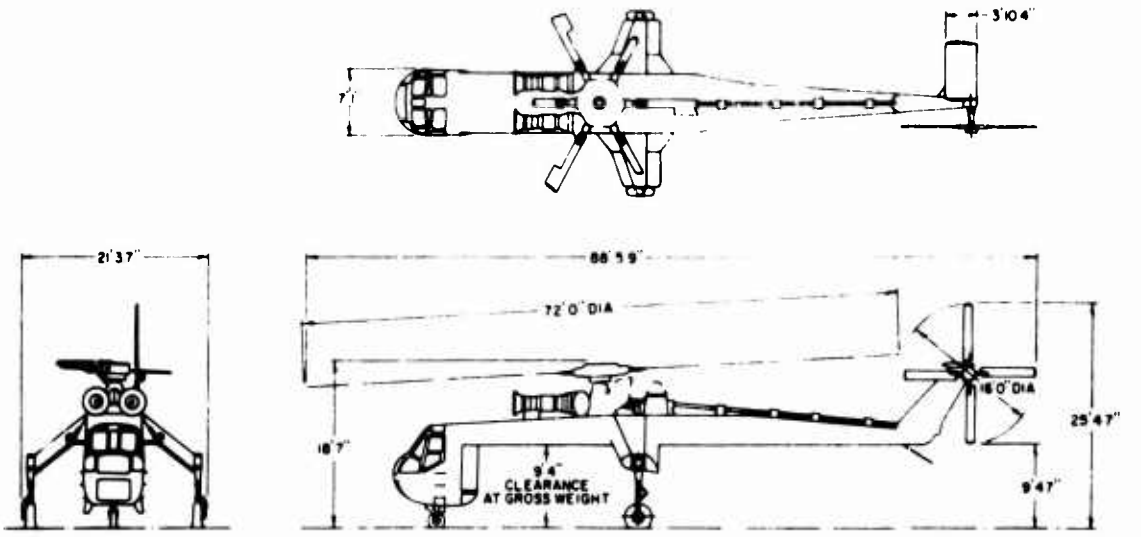

BASIC DATA		DESIGN LIMITS	
Main Rotor Dia.	72 ft	Normal Rated Power	*4000 shp
M.R. Solidity	0.08649	Transmission Limit Power	6600 hp
M.R. Blade Chord	1.629 ft	Max. Horiz. Flt. Airspeed	110 kn
No. of M.R. Blades	6	Limit Dive Speed	125.5 kn
Engines (two)	P&W JFTD-12A-4A	Limit Load Factor, N_z	2.26g
Max. Design Gr Wt	42000 lb		
Empty Weight	19234 lb		

* One Engine

Figure 1. CH-54A Three-View Drawing, Basic Data, and Design Limits.

OPERATIONAL MISSION PROFILES

ASSUMPTIONS FOR DEVELOPING OPERATIONAL MISSION PROFILES

Operational mission profiles were derived from the data in TR 70-73 for samples 1 and 2 (see Table I). Because the data as presented in TR 70-73 did not conform to standard Sikorsky flight regime definitions and since fatigue load levels on main and tail rotor head components are highly dependent on flight regime, a procedure was established to reclassify the field data into a more detailed mission profile. The four-segment breakdown of TR 70-73, namely, ascent, maneuver, descent, and steady state, was restructured into specific flight regimes consisting of ground, hover, sideward and rearward flight, ascent, descent, cruise, takeoff maneuvers, maneuvers, hoist, and gust. This detailed mission profile enabled a more accurate selection of flight conditions to be made from Sikorsky flight test records.

The reclassification of the TR 70-73 four-segment mission profile to the ten-segment profile used to develop fatigue loading spectra was derived from Tables VI (sample 1) and XLII (sample 2) by the following procedure:

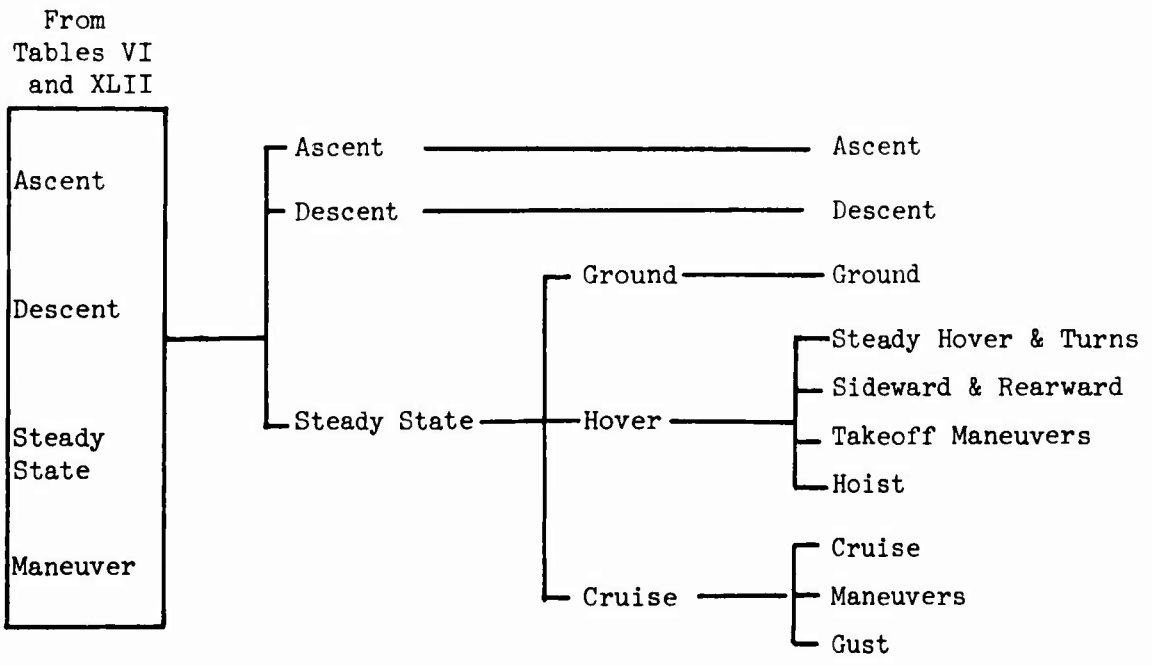

Three basic assumptions were made to derive the ascent, descent, and steady-state flight regimes from Table VI and Table XLII.

1) Ascent was assumed to be all positive climb rates.

2) Descent was assumed to be all negative climb rates except for the -300 ft/min climb category.

TABLE I. COMPARISON OF MISSION PROFILES

	Percentage of Aircraft Time			
	Sample 1 of TR 70-73	Sample 2 of TR 70-73	CH-54A Design Mission Profile	CH(Crane) Mission Profile of AR-56
Ground	0.295	0.186	2.110	1.000
Hover, Steady & Turns	5.880	7.015	21.385	16.000
Sideward & Rearward	0.653	0.779	2.175	1.500
Ascent	19.373	17.044	8.422	5.670
Descent	20.450	18.798	5.270	5.558
Cruise	52.790	55.753	53.240	61.234
Takeoff Maneuvers	0.159	0.100	0.020	1.330
Maneuvers	0.303	0.248	7.328	7.708
Hoist	0.049	0.045	-	-
Gust	0.048	0.032	-	-
Total	100.000	100.000	100.000	100.000

3) Steady state was assumed to be all time at -300 ft/min climb rate, since this category includes all time between -300 ft/min and +300 ft/min.

The detailed procedures by which the ascent, descent, and steady-state regimes were expanded to the ten-segment mission profile are explained in the following eleven steps:

1) Using Tables VI (sample 1) and XLII (sample 2) of TR 70-73, all time at -300 feet/min climb rate (all climb rates $\geq$ -300 to $<$ +300 ft/min) was considered to be cruise, hover, and ground operation regimes.

2) Data from the same tables were employed, and the ground operation regime was assumed to be the sum of the following:

   a) All time for -300 ft/min climb rate for C_T/σ = less and μ = 0.0, plus

   b) 25% of the time for -300 ft/min climb rate at C_T/σ = less and μ = less.

3) Data from the same tables were employed, and hover time, including sideward and rearward flight, was assumed to consist of

   a) All time for -300 ft/min climb rate and

      C_T/σ = .06, μ = less and μ = 0.0 and

      C_T/σ = .09, μ = less and μ = 0.0, plus

   b) 75% of the time for -300 ft/min climb rate, C_T/σ = less and μ = less.

4) The time for the cruise regime (including maneuver and gust N_z) was found by subtracting results of 2 plus 3 from 1 above.

5) Data from Tables VI and XLII were employed, and the ascent regime was established as all time at climb rates greater than +300 ft/min.

6) Data from the same tables were employed, and the descent regime was established as all time at climb rates less than -300 ft/min.

7) The maneuver N_Z occurrences were categorized as listed below in a, b, and c. The pulse times used in conjunction with these maneuvers are given in parentheses. These pulse times were developed from a study of Sikorsky flight test data and were conservatively assumed to be a rectangular pulse of peak N_Z versus time.

a) Hoist Maneuvers (3.0 sec) - The number of N_z occurrences for the hoist mission segment, as given in Tables XXVI (sample 1) and LXI (sample 2). Hoist N_z occurrences were recorded during hover while picking up or releasing payloads.

b) Takeoff Maneuvers (12 sec) - Based on Tables XXVI (sample 1) and LXI (sample 2), all N_z occurrences at $\mu \leq 0.0$ for the ascent, descent, maneuver, and steady-state mission segments.

c) Maneuvers During Cruise - All load factor (N_z) occurrences in Tables XXVI (sample 1) and LXII (sample 2) at $\mu > 0.0$ for the ascent, descent, maneuver, and steady-state mission segments. These maneuvers were classified as transitions, pull-ups, and turns using the following procedure:

i. For each mission segment (ascent, descent, steady state, and maneuver), all occurrences for $N_z \leq .8$ were considered negative ΔN_z transition maneuvers.

ii. All remaining maneuvers ($N_z \geq 1.2$) were distributed as follows:

a. The number of positive ΔN_z transition maneuvers equaled 50% of the number of negative ΔN_z transition maneuvers for all mission segments except steady state, where 25% was used.

b. The remaining positive ΔN_z occurrences were distributed between pull-ups (3 sec) and turns for the ascent, descent, and maneuver mission segments. All remaining positive ΔN_z occurrences for the steady-state mission segment were assumed to be turns.

iii. The total number of transition maneuvers obtained above were further subdivided into landing approaches (6 sec), lateral reversals (3 sec), and longitudinal reversals (3 sec). Similarly, the turn maneuvers were broken up into 90° turns (6 sec) and 180° turns (12 sec).

8) The maneuver times calculated in 7a and 7b above were subtracted from the hover time found in 3 above.

9) Ninety percent of the time obtained in 8 above was assumed to be steady hover including hover turns, and the remaining ten percent was assumed to be sideward and rearward flight.

10) For all mission segments, the gust N_z peaks in Tables XXV (sample 1) and LXI (sample 2) were assumed to occur during the cruise regime.

11) Net cruise time was calculated by subtracting the maneuver times of 7c and 10 from the time computed in 4 above.

GROSS WEIGHT, ALTITUDE, AND AIRSPEED DISTRIBUTION

Further breakdown of the operational mission profiles in Table I by gross weight, altitude, and airspeed was required. Since sample 1 and sample 2 were similar (see Table I), sample 1 was chosen for a detailed usage spectrum. To reduce the number of data points that would result from this breakdown, the full ranges of gross weight, altitude, and airspeed were grouped into several broader categories (see Figure 2).

Based on the histograms in TR 70-73, the percentage of time was determined for each of the three gross weight, four density altitude, and five airspeed categories. Using the assumptions discussed earlier for developing the mission profiles from TR 70-73, the total aircraft life (203.4 hours for sample 1) was divided into descent, cruise, and ascent by rate of climb (see Figure 2).

Figures 3, 4, and 5 illustrate the procedure used to calculate the time for each element of the detailed usage spectrum. Time ratios, noted by symbols in each of these three figures, were determined using the gross weight, altitude, and airspeed breakdowns from Tables IV and XL and the mission segments from Tables VI and XLII. All maneuver mission segment time, however, was combined into the cruise regime (R_C), since it represented only .46% of sample 1. (Maneuvers are discussed later.) These time ratios were multiplied together as indicated by the arrows in Figures 3, 4, and 5, and the results for each mission segment were summed to obtain the total time in each element of the detailed usage spectrum (see Table IV, presented in the "Fatigue Analysis" section).

For example, the total cruise time (T_C) for 25,000 pounds (W_1), sea level (H_1), and 70 knots (V_3) was

$$T_C = 100 \{(R_C \times W_1 \times H_1 \times V_3) \text{ for ascent}$$
$$+ (R_C \times W_1 \times H_1 \times V_3) \text{ for descent}$$
$$+ (R_C \times W_1 \times H_1 \times V_3) \text{ for steady state}$$
$$+ (R_C \times W_1 \times H_1 \times V_3)\} \text{ for maneuver} \qquad \text{Equation (1)}$$

(R_C, W_1, H_1, and V_3 are defined in Figure 3 and Table II)

Realistic mean ascent and descent airspeeds of 60 and 70 knots, respectively, were used throughout these regimes. Using this procedure, gross weight and altitude distributions were the only considerations for the ascent and descent regimes. The procedure was similar to that for the cruise regime, and the resulting calculations are reflected in Table IV.

Parameter	Data Category (TR 70-73)	Value Used In Study
Gross Weight (lb)	< 29000	25000
	≥ 29000 but < 37000	33000
	≥ 37000	39000
Density Altitude (ft)	< 1000	Sea Level
	≥ 1000 but < 2000	1000
	≥ 2000 but < 5000	2000
	≥ 5000	5000
Airspeed (KIAS)	< 40	20
	≥ 40 but < 60	40
	≥ 60 but < 80	70
	≥ 80 but < 95	85
	≥ 95	100
Rate of Climb (ft/min)	< -300	Descent
	≥ 300 but $< +300$	Cruise, Hover, Maneuver
	$\geq +300$	Ascent

Figure 2 . Grouping of Data from TR 70-73.

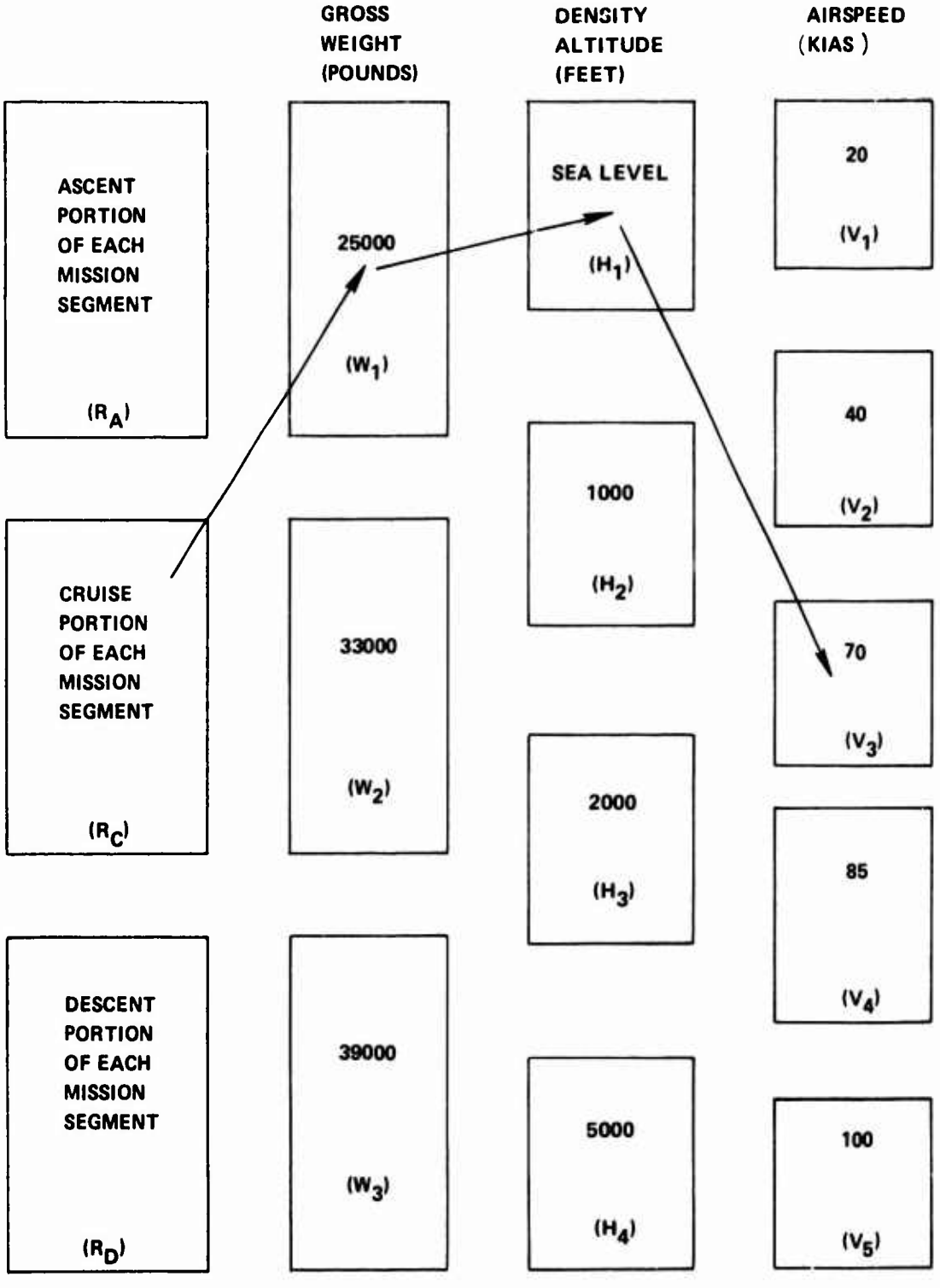

Figure 3. Parametric Distribution - Cruise (See Equation 1).

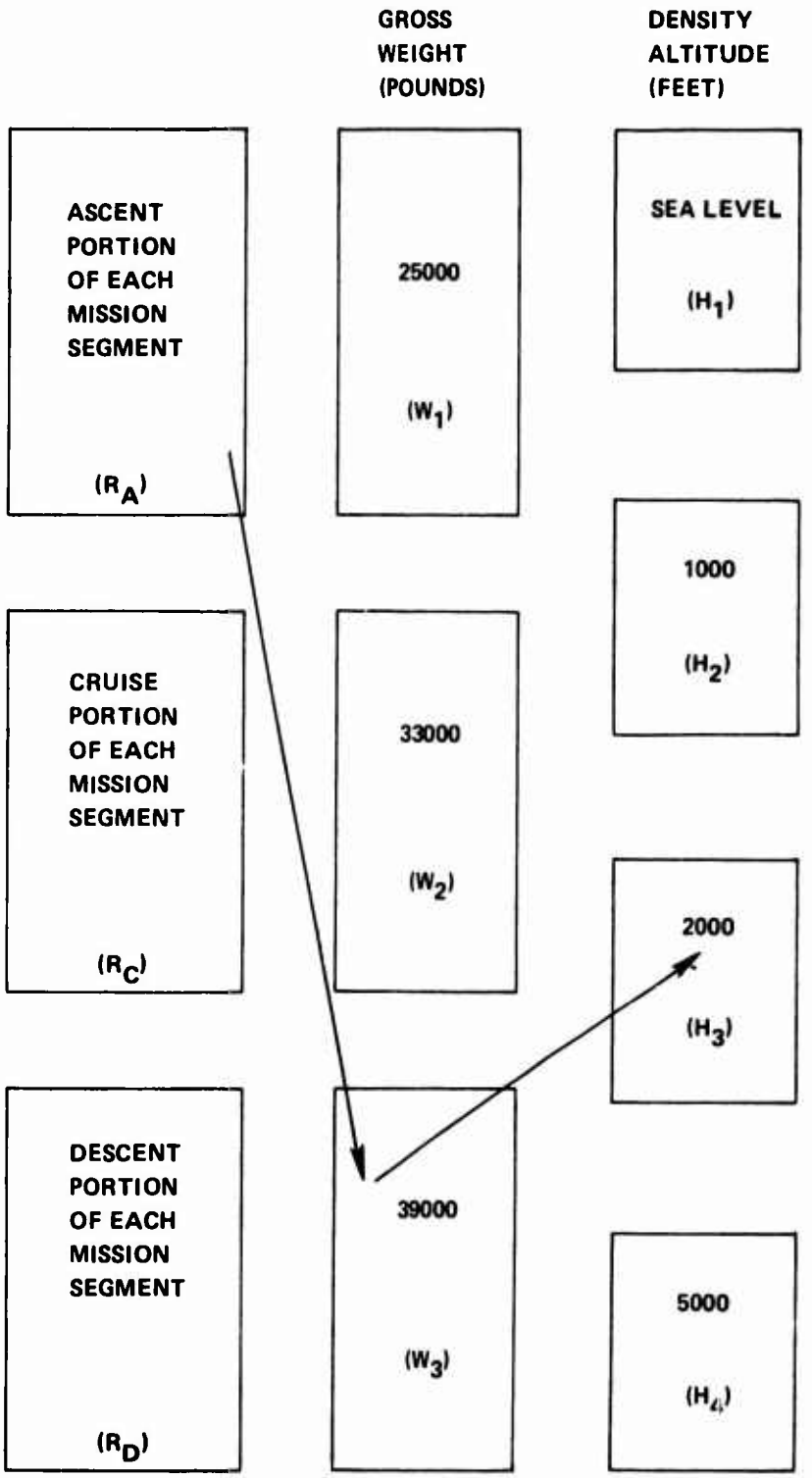

Figure 4. Parametric Distribution - Ascent (See Equation 2).

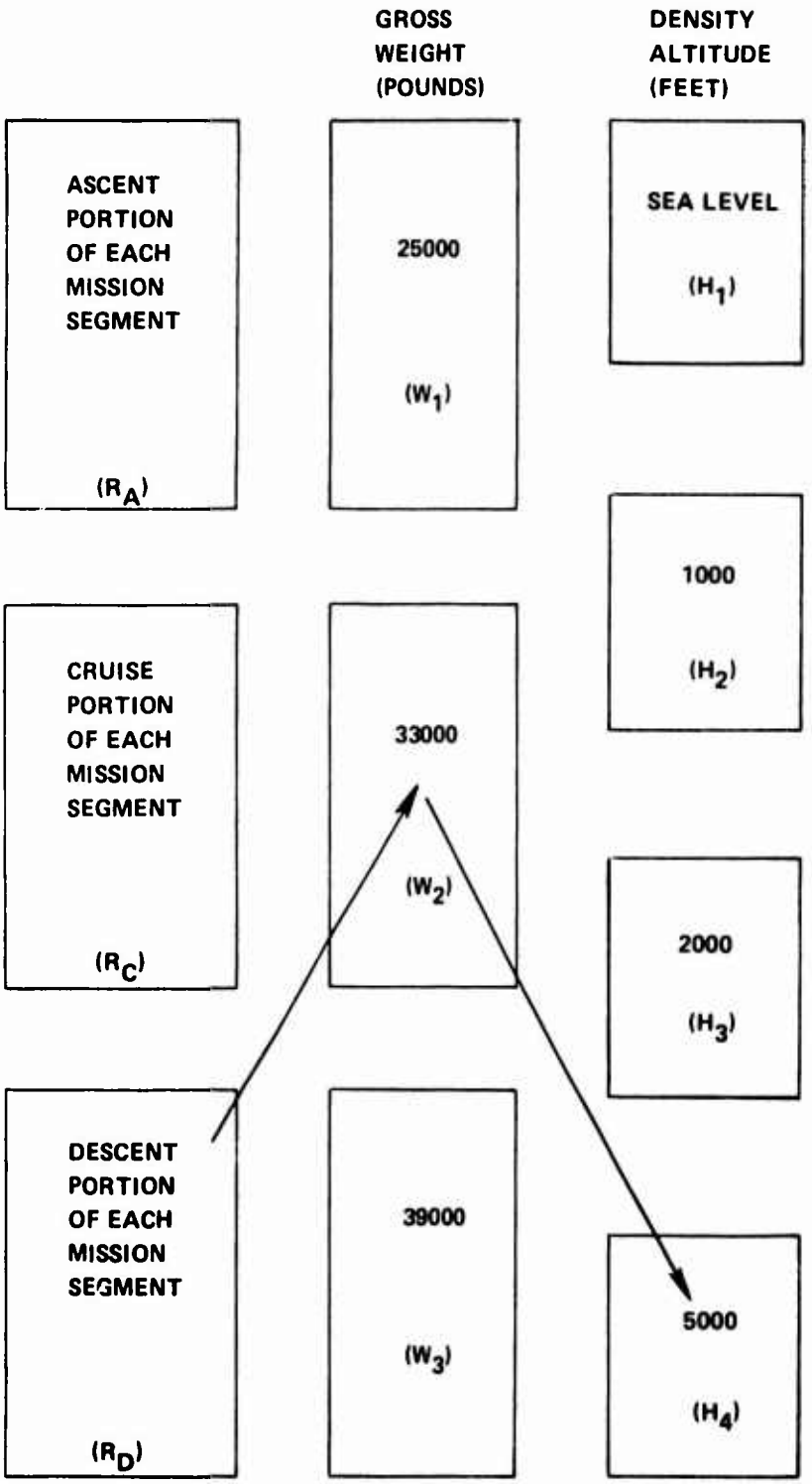

Figure 5. Parametric Distribution - Descent (See Equation 3).

TABLE II. TIME RATIOS FOR PARAMETRIC DISTRIBUTION

Time Ratio Symbol	Mission Segment (From TR 70-73)			
	Ascent	Descent	Steady State	Maneuver
R_A	.1766	.0044	.0127	0
R_D	.0030	.1880	.0135	0
R_C	.0682	.0836	.3749	.0046
W_1	.5125	.6343	.6428	1.000
W_2	.0799	.0979	.0972	0
W_3	.4076	.2678	.2601	0
H_1	.0097	.0115	.0070	0
H_2	.1024	.1267	.0475	0
H_3	.7844	.7491	.6090	.6364
H_4	.1036	.1127	.3365	.3636
V_1	.0873	.0855	.0097	0
V_2	.2437	.1478	.0454	0
V_3	.4667	.3491	.3469	.1034
V_4	.1705	.3065	.4524	.6988
V_5	.0318	.1112	.1456	.1979

For example, the total ascent time (T_A) for 39,000 (W_3) and 2,000 feet (H_3) was

$$T_A = 100 \{(R_A \times W_3 \times H_3) \text{ for ascent} + (R_A \times W_3 \times H_3) \text{ for descent} + (R_A \times W_3 \times H_3)\} \text{ for steady state} \qquad \text{Equation (2)}$$

(R_A, W_3, and H_3 are defined in Figure 4 and Table II.)

The total descent time (T_D) for 33,000 (W_2) and 5,000 feet (H_4) was

$$T_D = 100 \{(R_D \times W_2 \times H_4) \text{ for ascent} + (R_D \times W_2 \times H_4) \text{ for descent} + (R_D \times W_2 \times H_4)\} \text{ for steady state} \qquad \text{Equation (3)}$$

(R_D, W_2, and H_4 are defined in Figure 5 and Table II.)

COMPARISON OF CRANE MISSION PROFILES

Samples 1 and 2 of TR 70-73, the CH-54A design mission profile, and the CH (Crane) mission profile of AR-56 (Reference 2) were tabulated for comparative analysis (see Table I). Sample 1 correlated well with sample 2. There were significant discrepancies between several regimes of samples 1 and 2 and the CH-54A design mission profile and similarly between samples 1 and 2 and the CH (Crane) mission profile of AR-56. The CH (Crane) mission profile of AR-56 correlated well with the CH-54A design mission profile. The Crane profile is believed to be derived from the CH-54A design mission profile.

Ground Time

The ground time derived from TR 70-73 for the operational mission profiles (samples 1 and 2) was small compared with the CH-54A design spectrum and the CH (Crane) mission profile or AR-56. This time constituted 0.295% and 0.186%, respectively, of the total data sample times compared with 2.11% for the CH-54A design spectrum and 1.0% for the AR-56 spectrum. TR 70-73 indicated that the pilots used a switch in the cockpit to start the recording system that recorded in-flight data. The apparent ground time was probably recorded just prior to takeoff, whereas the design spectrum accounted for full warm-up.

Hover

Time in hover experienced under combat conditions in Southeast Asia differed significantly from CH-54A design hover time. These results are understandable. Under combat conditions, extended hovering is avoided to reduce vulnerability to enemy fire. The design spectrum, on the other hand, accounted for tasks involving extended periods of hover, including pilot training.

Ascent and Descent

Comparatively high ascent and descent times for the operational mission profile were influenced by the requirements of the combat environment. Field reports indicated that a typical ascent or descent maneuver was executed in a spiral fashion. Apparently, the pilot could make his approach to a drop zone at cruise altitude, staying out of rifle range as long as possible. He could then slowly make his descent while in relative safety from small-arms fire throughout his approach, since he would be close to an assumed friendly position. The same pattern would be used for ascent. Sikorsky field reports from Southeast Asia also indicated that most missions involved legs of 30 nautical miles or less. This would also tend to increase ascent and descent time.

Maneuvers

The low frequency of maneuvers during operation compared to design raised the question of whether raw data editing had eliminated large-radius, low-load-factor turns as maneuvers and, instead, categorized these turns as other mission segments, such as ascent and descent. As indicated in TR 70-73, only those load factors $\leq .80g$ and $\geq 1.20g$ were classified as N_z occurrences. This implied that turns at bank angles up to 33.5° were not included as maneuvers, since bank angle is a function of load factor. That is,

$$\phi = \cos^{-1} \frac{1}{N_z}$$

$$\phi = \cos^{-1} \frac{1}{1.2}$$

$$\phi = 33.5^{\circ}$$

where ϕ is aircraft bank angle.

Addition of these turns to the maneuver regime derived from operational data would produce a significant increase in maneuver time and bring it more in line with the CH-54A design mission profile.

EFFECTS OF ALTITUDE AND GROSS WEIGHT ON AIRSPEED

Gross weight, density altitude, and airspeed are important considerations in the fatigue design of helicopter dynamic components. These parameters have a direct influence on the magnitude of control loads and flapping and power requirements which, in turn, affect dynamic component replacement times. With this in mind, it becomes apparent that accurate knowledge of gross weight, altitude, and airspeed combinations would improve design mission profile development.

Data from TR 70-73 were compiled for sample 1, relating gross weight and density altitude to airspeed. Time was tabulated for airspeeds greater than or equal to 40 knots (IAS), neglecting any lesser speeds. This accounted for 87.2%. For this particular study, only 1000-foot, 2000-foot, and 5000-foot density altitudes were considered, accounting for 98.8% of the time at airspeeds greater than or equal to 40 knots. Gross weight groupings described in Figure 2 were also applicable to this study.

As a procedural example, the time for the 1000-foot density altitude was compiled for all gross weights less than 29,000 pounds and for the entire speed range $\geq$ 40 knots. The percentage of time for a particular speed within the overall speed range was then calculated. These individual percentages, totaling 100% of the time at airspeeds $\geq$ 40 knots, were accumulated beginning with the highest speed. The results were then plotted against true airspeed (Figures 6, 7, and 8), indicating the percentage of time that any given speed was equaled or exceeded for a particular density altitude and weight range. In this way, typical operating procedures could be shown graphically. In a similar manner, Figure 9 was developed to illustrate the percentage of time that any airspeed was equaled or exceeded for a particular weight range.

As noted in Figures 6, 7, 8, and 9, the indicated airspeeds of TR 70-73 were corrected to true airspeed, accounting for instrument error and density altitude (Table III). The results appearing in Figure 9 were further adjusted, using a weighted average, to combine the data for all altitudes into one mean altitude (2500 ft). This approach lent itself to a more meaningful comparison of gross weight versus airspeed.

Reduction of Southeast Asia flight loads data indicated that certain operating procedures were consistently practiced by U.S. Army pilots. One of the more predominant characteristics of crane helicopter operation was the airspeed-gross weight relationship. At aircraft gross weights greater than or equal to 37,000 pounds, the aircraft were flown very conservatively. High-gross-weight missions generally involved transport of bulky items by the single-point hoist system, making low-speed flying essential for maintaining safe control of the slung load.

Figure 9 confirms that heavy loads were flown at relatively low speeds, especially compared with gross weights below 29,000 pounds. For this weight range, the aircraft would not have been carrying any external cargo,

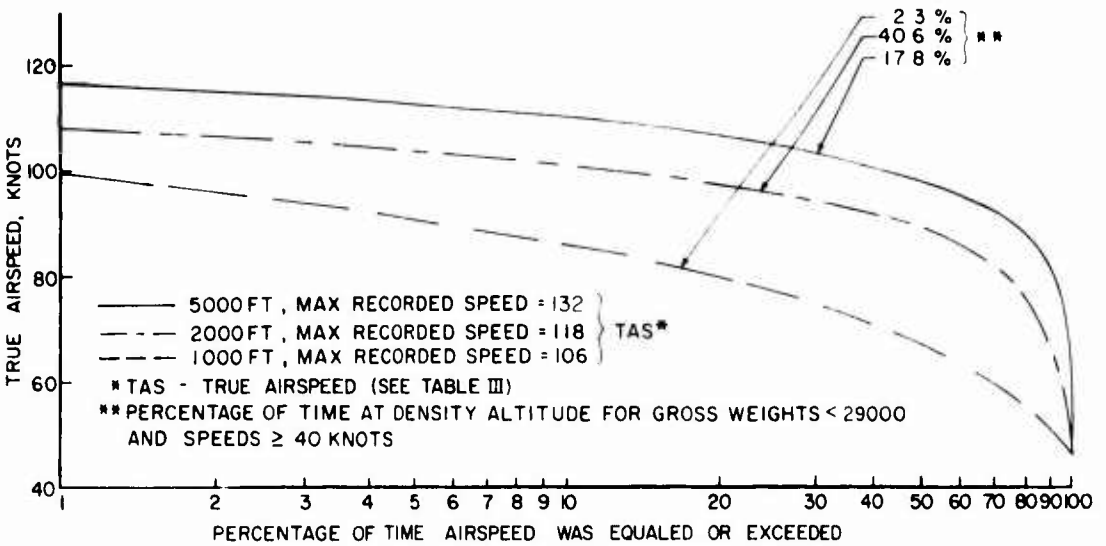

Figure 6. True Airspeed Vs. Cumulative Percentage of Time for Gross Weights Less Than 29,000 Pounds.

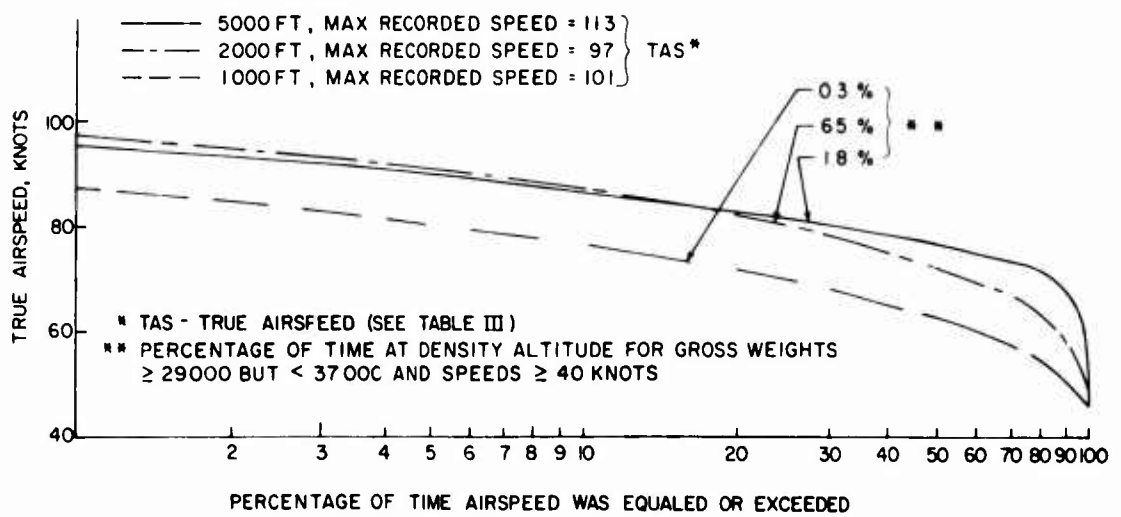

Figure 7. True Airspeed Vs. Cumulative Percentage of Time for Gross Weights Greater Than or Equal to 29,000 Pounds but Less Than 37,000 Pounds.

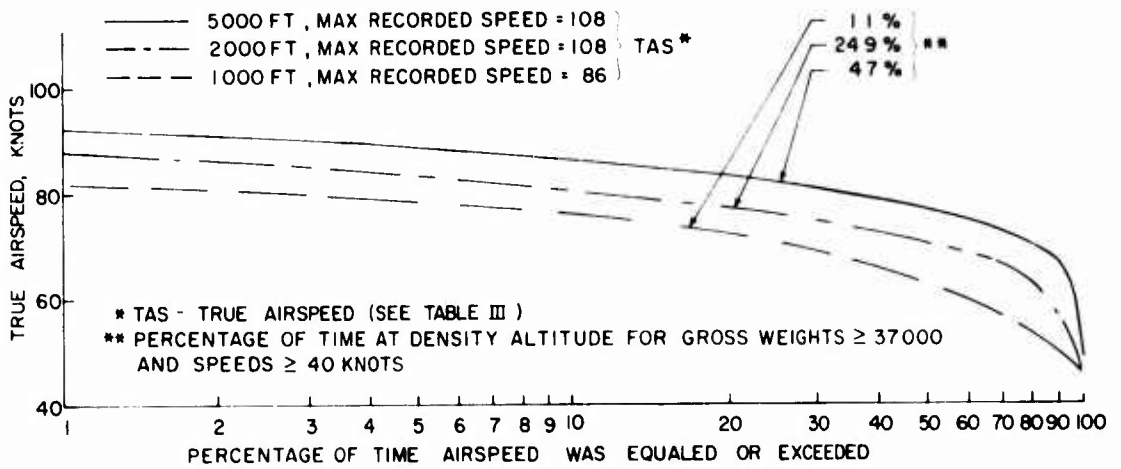

Figure 8. True Airspeed Vs. Cumulative Percentage of Time for Gross Weights Greater Than or Equal to 37,000 Pounds.

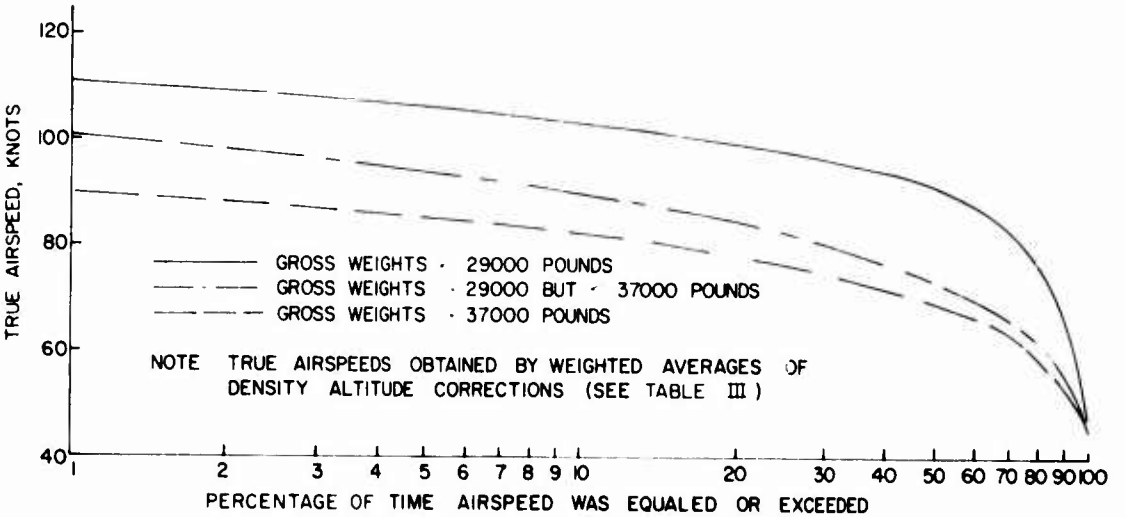

Figure 9. True Airspeed Vs. Cumulative Percentage of Time for Gross Weight Ranges and a Mean Density Altitude of 2,500 Feet.

TABLE III. INDICATED AIRSPEED CORRECTED TO TRUE AIRSPEED

Indicated Airspeed (kn)	Calibrated * Airspeed (kn)	True Airspeed (kn) **		
		1000 Ft	2000 Ft	5000 Ft
40	45	46	46	48
60	62.5	63.5	64	67
65	67	69	69	72
70	71	72	73	76
75	75.5	77	78	81
80	80	81	82	86
85	84.5	86	87	91
90	89	90	92	97
95	94	95.5	97	101
100	99.5	101	103	108
105	104.5	106	108	113
110	110	112	113	118
115	115	117	118	124
120	123	125	127	132

*Reference 3

**True Airspeed = $\frac{\text{Calibrated Airspeed}}{\sqrt{\rho/\rho_o}}$

Where $\sqrt{\rho/\rho_o}$ = .985 @ 1000 Ft, .971 @ 2000 Ft and .928 @ 5000 Ft

but would have been loaded to maximum fuel capacity or less. Adjusted for true airspeed corrections at a mean altitude of 2,500 feet, the curves indicate that, for a given speed, considerably more time was spent at gross w ights less than 29,000 pounds than at weights involving a payload. As an example, for true airspeeds of 80 knots, 80% of the time spent below 29,000 pounds was flown at or above this speed compared to only 15% for weights at or above 37,000 pounds. Examining the curves from another viewpoint, 50% of the time at gross weights less than 29,000 pounds was spent at or above airspeeds of 91 knots (TAS), while the equivalent time at gross weights greater than or equal to 37,000 pounds equaled or exceeded only 69 knots (TAS).

These facts are important considerations in the development of a speed spectrum for cruise and maneuvers. There is a tendency to be overly conservative in establishing an airspeed vs. gross weight distribution; however, the data compiled for this report may help promote a more accurate approach to this problem.

Another important aspect of mission profile development is the relationship of density altitude to aircraft speed. It is common design practice to develop fatigue load spectra at various density altitudes above sea level standard for speeds up to the limit dive speed at the design gross weight. From the standpoint of control loads, this approach could be excessively conservative for crane helicopter design. Analyzing control loads for high-speed flight at high density altitudes creates high loading conditions. If a more rational approach could be formulated for determining practical density altitude, gross weight, and airspeed combinations, component design improvements could be realized.

Figures 6, 7, and 8 help to illustrate the relationships among altitude, gross weight, and airspeed. True airspeed vs. cumulative percentage of time for each altitude as a function of the entire forward speed range has also been provided in each figure. With this information, the percentage of time that an airspeed was equaled or exceeded can be calculated for any combination of altitude and gross weight.

For example, to determine the percentage of time spent at or above 80 knots for gross weights greater than 37,000 pounds and a density altitude of 5,000 feet or more, Figure 8 would be used. From the figure, 32% of the time for 5,000 feet and 37,000 pounds was spent at or above 80 knots. Relating this percentage to the total aircraft life spent in forward flight, the result is .32 x 4.7% = 1.5%. This approach provides a useful tool for future mission profile development.

FATIGUE ANALYSIS

SELECTION OF COMPONENTS

Initially, the main rotor pitch control horn, main rotor shaft, and tail rotor spindle were selected for fatigue analysis. The intention was to compare replacement times based on the operational mission profile with those established during design. However, the analysis showed that the replacement time based on the operational mission profile for both the main rotor pitch control horn and tail rotor spindle was "unlimited," as was the case under the existing Army replacement time schedule. Subsequently, three additional components were evaluated, using the operational fatigue spectrum: the main rotor hub, magnesium main rotor head spacer (currently being phased out for reasons explained later in the text), and the newly incorporated aluminum main rotor head spacer.

SELECTION OF FLIGHT LOADS

Flight test results on the CH-54A were available from four Sikorsky engineering reports (References 3, 4, 5, and 6). Flight loads were selected by matching specific flight regimes of the operational mission profile with actual flight demonstrated maneuvers. When operational flight regimes could not be matched exactly by flight test conditions, conservative alternative conditions were used. When two or more loads were available from flight test data for a particular regime, the highest load was used. When a peak load appeared in the flight test records for conditions of low intensity (low airspeed, altitude, or gross weight conditions), this same load was used for similar conditions of high intensity (high airspeed, altitude, or gross weight conditions). In other words, for reasons such as gust response or high transient pilot inputs, there were cases when peak loads for low-intensity conditions exceeded the highest recorded loads for high-intensity conditions. Table IV summarized the detailed usage spectra and corresponding critical flight loads that were used for component evaluation. Mean and working S/N curves for each component were used to determine damaging flight load levels. Gross weight, center of gravity, altitude, and airspeed were considered in compiling conditions for each component. Only those conditions with corresponding flight test loads exceeding the working strength of the component at 10^8 cycles were considered for the operational fatigue analysis.

No hoist conditions were simulated during the CH-54A flight test program to determine rotor loads. Therefore, damaging loads experienced during hover regimes were applied to hoist maneuvers.

TABLE IV. OPERATIONAL FATIGUE SPECTRA

	% Time	Gross Weight (lb)	Altitude (ft)	N_Z (g)	Airspeed (kn)	P_V (lb)	M_S (in.-lb x 10^{-6})	M_H (in.-lb x 10^{-6})
Ground	.295	25000	S.L.	1.0	0	<980	<.0187	<.35
Hover -	.03206	25000	S.L.					
Steady, Turns	.30259	25000	1000					
	2.48693	25000	2000					
	.75282	25000	5000					
	.00488	33000	S.L.					
	.04605	33000	1000					
	.37847	33000	2000					
	.11457	33000	5000					<.35
	.01580	39000	S.L.					.423
	.14918	39000	1000					
	1.22604	39000	2000					
	.37114	39000	5000		0			.423
Hover -	.00356	25000	S.L.		30			<.35
Sideward and	.03362	25000	1000					
Rearward	.27633	25000	2000					
	.08365	25000	5000					
	.00054	33000	S.L.					
	.00512	33000	1000					
	.04205	33000	2000					
	.01273	33000	5000					<.35
	.00176	39000	S.L.					.438
	.01658	39000	1000					
	.13623	39000	2000					
	.04124	39000	5000	1.0	30	<980	<.0187	.438

TABLE IV - Continued

Regime	% Time	Gross Weight (lb)	Altitude (ft)	N_Z (g)	Airspeed (kn)	P_V (lb)	M_S (in.-lbx10^{-6})	M_H (in.-lbx10^{-6})
Ascent	.09671	25000	S.L.	1.0	60	< 980	<.0187	<.35
	1.00094	25000	1000					
	7.80564	25000	2000					
	1.24381	25000	5000					
	.01505	33000	S.L.					
	.15581	33000	1000					
	1.21427	33000	2000					
	.19257	33000	5000					
	.07349	39000	S.L.					
	.76772	39000	1000					
	5.93572	39000	2000					
	.87018	39000	5000		60			
Descent	.14469	25000	S.L.		70			
	1.56782	25000	1000					
	9.58186	25000	2000					
	1.65184	25000	5000					
	.02230	33000	S.L.					
	.24187	33000	1000					
	1.47744	33000	2000					
	.25405	33000	5000					<.35
	.06152	39000	S.L.					.391
	.66707	39000	1000					.391
	4.08119	39000	2000					.391
	.69821	39000	5000	1.0	70	< 980	<.0187	.391

TABLE IV - Continued

Regime	% Time	Gross Weight (lb)	Altitude (ft)	N_Z (g)	Airspeed (kn)	P_V (lb)	M_S (in.-lbx10^{-6})	M_H (in.-lbx10^{-6})
Cruise	.00981	25000	S.L.	1.0	20	<980	<.0187	<.35
	.02410	↑	↕	↑	40	↑	↑	↑
	.09561	↕	↕	↕	70	↕	↕	↕
	.10079	↕	↓	↕	85	↕	↕	↕
	.03239	↕	S.L.	↕	100	↕	↕	↕
	.09824	↕	1000	↕	20	↕	↕	↕
	.23528	↕	↑	↕	40	↕	↕	↕
	.79227	↕	↕	↕	70	↕	↕	↕
	.78167	↕	↓	↕	85	↕	↕	↕
	.25270	↕	1000	↕	100	↕	↕	↕
	.72132	↕	2000	↕	20	↕	↕	↕
	1.90886	↕	↑	↕	40	↕	↕	↕
	7.72198	↕	↕	↕	70	↕	↕	↕
	8.39366	↕	↓	↕	85	↕	↕	↕
	2.67185	↕	2000	↕	100	↕	↕	↕
	.16175	↕	5000	↕	20	↕	↕	↕
	.54486	↕	↑	↕	40	↕	↕	↕
	3.20401	↕	↕	↕	70	↕	↕	↕
	3.99740	↕	↓	↕	85	↕	↕	↕
	1.27216	25000	5000	↕	100	↕	↕	↕
	.00149	33000	S.L.	↕	20	↕	↕	↕
	.00383	↑	↑	↕	40	↕	↕	↕
	.01458	↕	↕	↕	70	↕	↕	↕
	.01530	↕	↓	↕	85	↕	↕	↕
	.00492	↕	S.L.	↕	100	↕	↕	↕
	.01541	↕	1000	↕	20	↕	↕	↕
	.03678	↕	↑	↕	40	↕	↕	↕
	.12229	↕	↕	↕	70	↕	↕	↕
	.11961	↕	↓	↕	85	↕	↕	↕
	.03850	33000	1000	1.0	100	<980	<.0187	<.35

TABLE IV - Continued

Regime	% Time	Gross Weight (lb)	Altitude (ft)	N_Z (g)	Airspeed (kn)	P_V (lb)	M_S (in.-lbx10^{-6})	M_H (in.-lbx10^{-6})
Cruise (cont.)	.11137	33000	2000	1.0	20	<980	<0.187	<.35
	.29555	↕	↕	↕	40	↕	↕	↕
	1.18265	↕	↕	↕	70	↕	↕	↕
	1.26483	↕	↕	↕	85	↕	↕	↕
	.40477	↕	2000	↕	100	↕	↕	↕
	.02476	↕	5000	↕	20	↕	↕	↕
	.08307	↕	↕	↕	40	↕	↕	↕
	.48396	↕	↕	↕	70	↕	↕	↕
	.59262	↕	↕	↕	85	↕	↕	↕
	.19051	33000	5000	↕	100	↕	↕	↕
	.00521	39000	S.L.	↕	20	↕	↕	↕
	.01348	↕	↕	↕	40	↕	↕	↕
	.04523	↕	↕	↕	70	↕	↕	↕
	.04335	↕	↕	↕	85	↕	↕	↕
	.01365	↕	S.L.	↕	100	↕	↕	↕
	.05361	↕	1000	↕	20	↕	↕	↕
	.13230	↕	↕	↕	40	↕	↕	↕
	.39256	↕	↕	↕	70	↕	↕	↕
	.34504	↕	↕	↕	85	↕	↕	↕
	.10799	↕	1000	↕	100	↕	↕	↕
	.39171	↕	2000	↕	20	↕	↕	↕
	1.04776	↕	↕	↕	40	↕	↕	↕
	3.65600	↕	↕	↕	70	↕	↕	↕
	3.57121	↕	↕	↕	85	↕	↕	↕
	1.12009	↕	2000	↕	100	↕	↕	↕
	.07870	↕	5000	↕	20	↕	↕	↕
	.25680	↕	↕	↕	40	↕	↕	↕
	1.36004	↕	↕	↕	70	↕	↕	↕
	1.61089	↕	↕	↕	85	↕	↕	↕
	.51479	39000	5000	1.0	100	<980	<.0187	<.35

TABLE IV - Continued

Regime	% Time	Gross Weight (lb)	Altitude (ft)	N_Z (g)	Airspeed (kn)	P_V (lb)	M_S (in.-lbx10^{-6})	M_H (in.-lbx10^{-6})
Takeoff	.00492	25000	S.L.	1.2	0	<980	<.0187	<.35
	.00492	↕	1000	1.3	↕	↕	↕	↕
	.04100	↕	1000	1.2	↕	↕	↕	↕
	.00164	↕	2000	1.4	↕	↕	↕	↕
	.00328	↕	2000	1.3	↕	↕	↕	↕
	.08200	25000	2000	1.2	↕	↕	↕	↕
	.00328	33000	1000	1.2	↕	↕	↕	↕
	.00164	39000	S.L.	1.2	↕	↕	↕	↕
	.00984	39000	1000	1.2	↕	↕	↕	↕
	.00656	39000	2000	1.2	↕	↕	↕	↕
Hoist	.00082	25000	S.L.	1.3	↕	↕	↕	↕
	.00205	↕	S.L.	1.2	↕	↕	↕	↕
	.00041	↕	1000	1.5	↕	↕	↕	↕
	.00082	↕	↕	1.4	↕	↕	↕	↕
	.00369	↕	↕	1.3	↕	↕	↕	↕
	.00532	↕	↕	1.2	↕	↕	↕	↕
	.00205	↕	1000	0.7	↕	↕	↕	↕
	.00164	↕	2000	1.3	↕	↕	↕	↕
	.00942	↕	2000	1.2	↕	↕	↕	↕
	.00041	25000	2000	0.5	↕	↕	↕	↕
	.00041	33000	S.L.	1.2	↕	↕	↕	↕
	.00041	↕	1000	1.4	↕	↕	↕	↕
	.00082	↕	↕	1.3	↕	↕	↕	↕
	.00082	↕	↕	1.2	↕	↕	↕	↕
	.00082	33000	1000	0.7	0	<980	<.0187	<.35

TABLE IV - Continued

Regime	% Time	Gross Weight (lb)	Altitude (ft)	N_Z (g)	Airspeed (kn)	P_V (lb)	M_S (in.-lbx10^{-6})	M_H (in.-lbx10^{-6})
Hoist (cont)	.00041	39000	S.L.	1.4	0	<.980	<.0187	.423
	.00041		S.L.	1.2				
	.00041		1000	1.8				
	.00041			1.6				
	.00246			1.3				
	.00409			1.2				
	.00082		1000	0.7				
	.00041		2000	1.5				
	.00205		2000	1.3				
	.00655		2000	1.2				
	.00082	39000	2000	0.7	0			.423
Maneuver-Lndg. Approach	.00082	25000	S.L.	1.2	40			<.35
	.00082		1000	1.2	20			
	.00082		1000	0.7	40			
	.00082		1000	1.2	40			
	.00246		1000	1.2	70			
	.00082		2000	1.3	20			
	.00082			0.7	40			
	.01312			0.7	70			
	.00082			1.3	40			
	.00164			1.2	40			
	.00164			1.3	70			
	.00656		2000	1.2	70			
	.00328	25000	5000	0.7	70			
	.00082	33000	2000	1.2	70			
	.00082	39000	2000	1.2	40			
	.00164	39000	2000	0.7	70			
	.00164	39000	2000	1.2	70	<.980	<.0187	<.35

TABLE IV - Continued

Regime	% Time	Gross Weight (lb)	Altitude (ft)	N_Z (g)	Airspeed (kn)	P_V (lb)	M_S (in.-lbx10^{-6})	M_H (in.-lbx10^{-6})
Maneuver-Long. (cont.) Rev.	.00041	25000	1000	1.2	20	<980	<.0187	.698
	.00041	↑	↑	1.2	40	↑	↑	↑
	.00082	↕	↕	1.2	70	↕	↕	↕
	.00082	↓	↓	1.2	85	↓	↓	↓
	.00041		1000	1.3	85			
	.00205		2000	1.2	40			
	.00041		↑	1.2	70			
	.00041		↕	1.3	70			
	.00041		↕	0.6	85			
	.00123		↕	1.3	85			
	.00533		↓	0.7	100			
	.00041		2000	0.6	100			
	.00041		5000	0.6	85			
	.00492		5000	0.7	85			
	.00205		5000	0.7	100			.698
Maneuver-Lat. Rev.	.00041		1000	1.2	40			<.35
	.00123		1000	1.2	70			<.35
	.00041		1000	1.2	85			<.35
	.00205		2000	1.2	40			.357
	.00041		↑	1.3	40			↑
	.00082		↕	1.2	70			↕
	.00041		↕	1.3	70			↕
	.00041		↕	0.6	85			↕
	.00943		↕	0.7	85			↕
	.00123		↕	1.3	85			↕
	.00041		↕	0.5	100			↕
	.00533		2000	0.7	100			↕
	.00492		5000	0.7	85			↕
	.00246	25000	5000	0.7	100	<980	<.0187	.357

TABLE IV - Continued

Regime	% Time	Gross Weight (lb)	Altitude (ft)	N_Z (g)	Airspeed (kn)	P_V (lb)	M_S (in.-lbx10^{-6})	M_H (in.-lbx10^{-6})
Maneuver-Turns (Cont.)	.00164	25000	2000	1.4	40	<980	<.0187	<.35
	.03772	↕	↕	1.2	70	↕	↕	↕
	.00246			1.4	70			
	.09184			1.2	85			
	.00164			1.5	85			
	.02624	25000		1.2	100			
	.00410	39000	2000	1.2	70			
	.00082	25000	5000	1.2	70			
	.00656	25000	5000	1.2	85			
	.00656	25000	5000	1.2	100			
Maneuver Pull-ups	.00492	25000	2000	1.2	70			
	.00041	↕	↕	1.4	70			
	.00041			1.5	70			
	.01189			1.2	85			↓
	.00328	25000		1.2	100			<.35
	.00041	39000		1.2	70			.395
	.00041	39000	2000	1.4	85			.395
	.00082	25000	5000	1.2	85			<.35
	.00082	25000	5000	1.2	100	<980	<.0187	<.35

TABLE IV - Concluded

Regime	% Time	Gross Weight (lb)	Altitude (ft)	N_Z (g)	Airspeed (kn)	P_V (lb)	M_S (in.-lbx10^{-6})	M_H (in.-lbx10^{-6})
Gusts	.00055	25000	2000	1.2	40	<980	<.0187	<.35
	.00027	↑	↑	0.7	40	↑	↑	↑
	.00437	↑	↑	1.2	70	↑	↑	↑
	.00273	↑	↑	0.7	70	↑	↑	↑
	.00027	↑	↑	0.6	70	↑	↑	↑
	.00055	↑	↑	1.3	85	↑	↑	↑
	.00764	↑	↑	1.2	85	↑	↑	↑
	.00710	↑	↑	0.7	85	↑	↑	↑
	.00083	↑	↑	0.6	85	↑	↑	↑
	.00027	↑	↑	1.3	100	↑	↑	↑
	.00355	↑	↑	1.2	100	↑	↑	↑
	.00328	↑	↑	0.7	100	↑	↑	↑
	.00027	↑	2000	0.6	100	↑	↑	↑
	.00027	↑	5000	1.2	70	↑	↑	↑
	.00027	↑	↑	1.3	85	↑	↑	↑
	.00246	↑	↑	1.2	85	↑	↑	↑
	.00437	↑	↑	0.7	85	↑	↑	↑
	.00083	↑	↑	0.6	85	↑	↑	↑
	.00191	↑	↑	1.2	100	↑	↑	↑
	.00328	↑	↑	0.7	100	↑	↑	↑
	.00027	25000	5000	0.6	100	↑	↑	↑
	.00027	39000	2000	1.2	40	↑	↑	↑
	.00083	↑	↑	1.2	70	↑	↑	↑
	.00027	↑	↑	1.2	85	↑	↑	↑
	.00027	↑	2000	0.7	85	↑	↑	↑
	.00055	↑	5000	1.2	70	↑	↑	↑
	.00027	39000	5000	0.7	70	<980	<.0187	<.35

REPLACEMENT TIME CALCULATIONS

Appropriate fatigue design load parameters were selected from CH-54A flight test results and paired with corresponding flight conditions of the operational mission profile. The related percentages of time, which were derived from Southeast Asia field data, were used together with these parameters to calculate replacement times.

$$\text{Replacement Time} = \frac{100}{D}$$

where

$$D = \sum_{i=1}^{i=n} d_i$$

and

$$d_i = \frac{\% \text{ Time}}{\frac{\text{Allowable Cycles}}{\text{Cycles/Hour}}}$$

The allowable cycles at each load level were obtained from appropriate working S/N curves. Cycles per hour were calculated, assuming a constant rotor speed of 185 rpm and one load cycle per rotor revolution.

COMPONENT EVALUATION

(a) Main Rotor Pitch Control Horn

The mean and working S/N curves for the main rotor pitch control horn (Figure 10) were obtained from Reference 7.

As indicated, the maximum vibratory pushrod load encountered during any flight regime of the operational mission profile does not intersect the working S/N curve. Therefore, no fatigue damage is incurred, resulting in an "unlimited" replacement time for the control horn.

Because this does not represent any change from the existing Army replacement time, it was decided to evaluate an alternative component. The main rotor hub was chosen, since it has a relatively low replacement time of 750 hours. This evaluation is made in section (d) below.

(b) Main Rotor Shaft

The mean and working S/N curves for the main rotor shaft (Figure 11) were obtained from Reference 8. Table V presents the replacement time calculations.

Head moments in Table IV were calculated as shown on page 33, using the upper shaft bending stresses and the blade flapping angles recorded in the flight test reports.

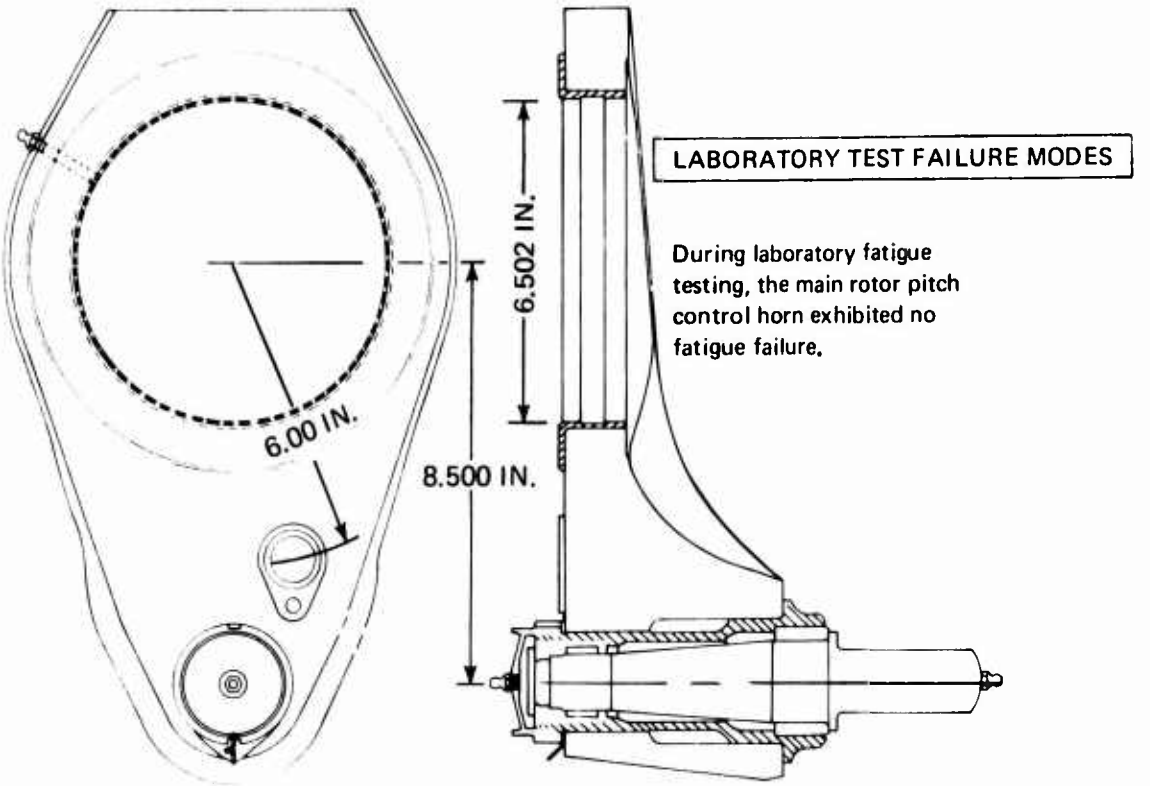

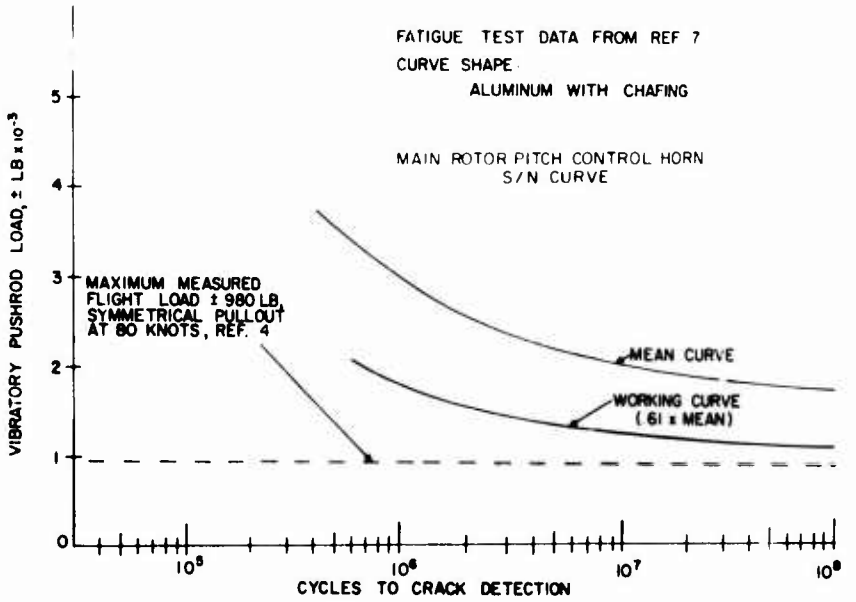

Figure 10. Main Rotor Pitch Control Horn Fatigue Substantiation Data.

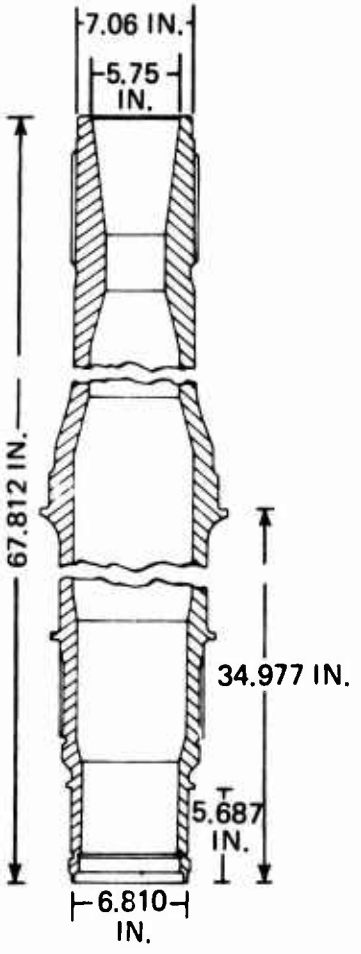

FATIGUE TEST FAILURE MODE

Failure Mode - Cracking occurred across the lower portion of the upper splines, extending almost completely around the circumference. Cracks also extended longitudinally. Fretting and galling of the upper splines were also evident, concentrated mainly at the ends.

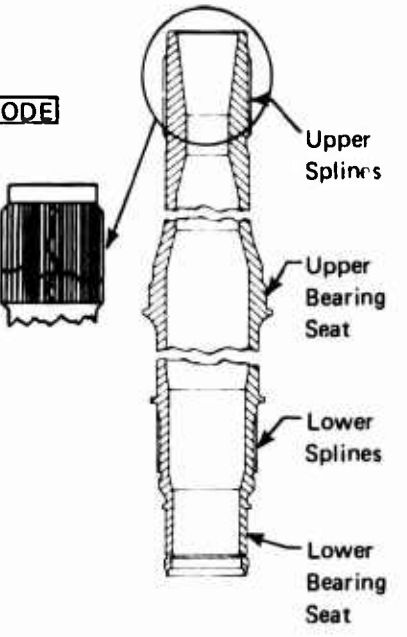

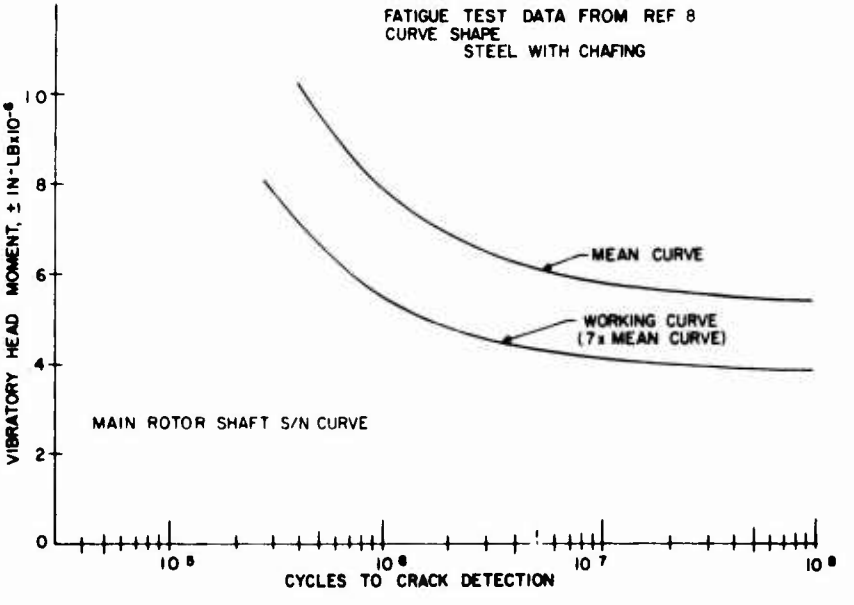

Figure 11. Main Rotor Shaft Fatigue Substantiation Data.

TABLE V. MAIN ROTOR SHAFT REPLACEMENT TIME CALCULATION

M_H (in. -lb x 10^{-6}) Ref. Table IV	Σ % Time Ref. Table IV	Allowable Cycles x 10^{-6} Ref. Fig. 11	Allowable Hours *	Damage per 100 Hours
.423	1.7808	4.8	432	.00412
.438	.1958	3.8	342	.00057
.391	5.508	14.0	1261	.00437
.698	.0205	.425	38	.00053
.395	.00082	11.8	1063	0
			Total Damage/100 Hours	.00959

Replacement Time = $\frac{100}{.00959}$ = 10,400 Hours

* Assumes a main rotor speed of 185 rpm and one cycle per revolution.

$$F_G = \frac{M_G}{Z}$$

and

$$M_G = M_H + M_B$$

$$= M_H + T_{MR} \times L \times \frac{\beta}{57.3}$$

where F_G = Bending stress on main rotor shaft at strain gage location, psi

M_G = Net bending moment on main rotor shaft at strain gage location, in.-lb

Z = Main rotor shaft section modulus at strain gage location, $in.^3$

M_H = Bending moment at centerline of main rotor hub, in.-lb

M_B = Bending moment on main rotor shaft at strain gage location due to blade flapping, in.-lb

T_{MR} = Main rotor axial thrust, lb

L = Distance from centerline of hub to strain gage location on main rotor shaft, in.

β = Main rotor flapping angle, deg

The calculated replacement time of 10,400 hours is compared with existing replacement times in Table IX.

(c) Tail Rotor Spindle

The working S/N curves for the four designs of the tail rotor spindle used at one time or another on the CH-54A aircraft were obtained from References 9 and 10 and are presented in Figure 12. It should be noted that neither the -041 nor the -044 spindle is in service at the present time.

As shown in Figure 12, the maximum vibratory spindle moment encountered during the operational mission profile does not intersect the working S/N curve for either the -046 or -047 tail rotor spindle (see Table X for part descriptions). As a result, no fatigue damage occurs, and an "unlimited" replacement time is obtained. Since this does not represent any change from the design replacement time shown in Table IX, it was decided to evaluate the fatigue life of the main rotor spacers.

(d) Main Rotor Hub

The mean and working S/N curves for the main rotor hub, shown in Figure 13, were taken from Reference 8. The replacement time calculation, based upon the operational mission profile, is shown in Table VI. As can be seen from Table IX, the calculated replacement time of 7,700 hours is more than 10 times the FAA-approved replacement time.

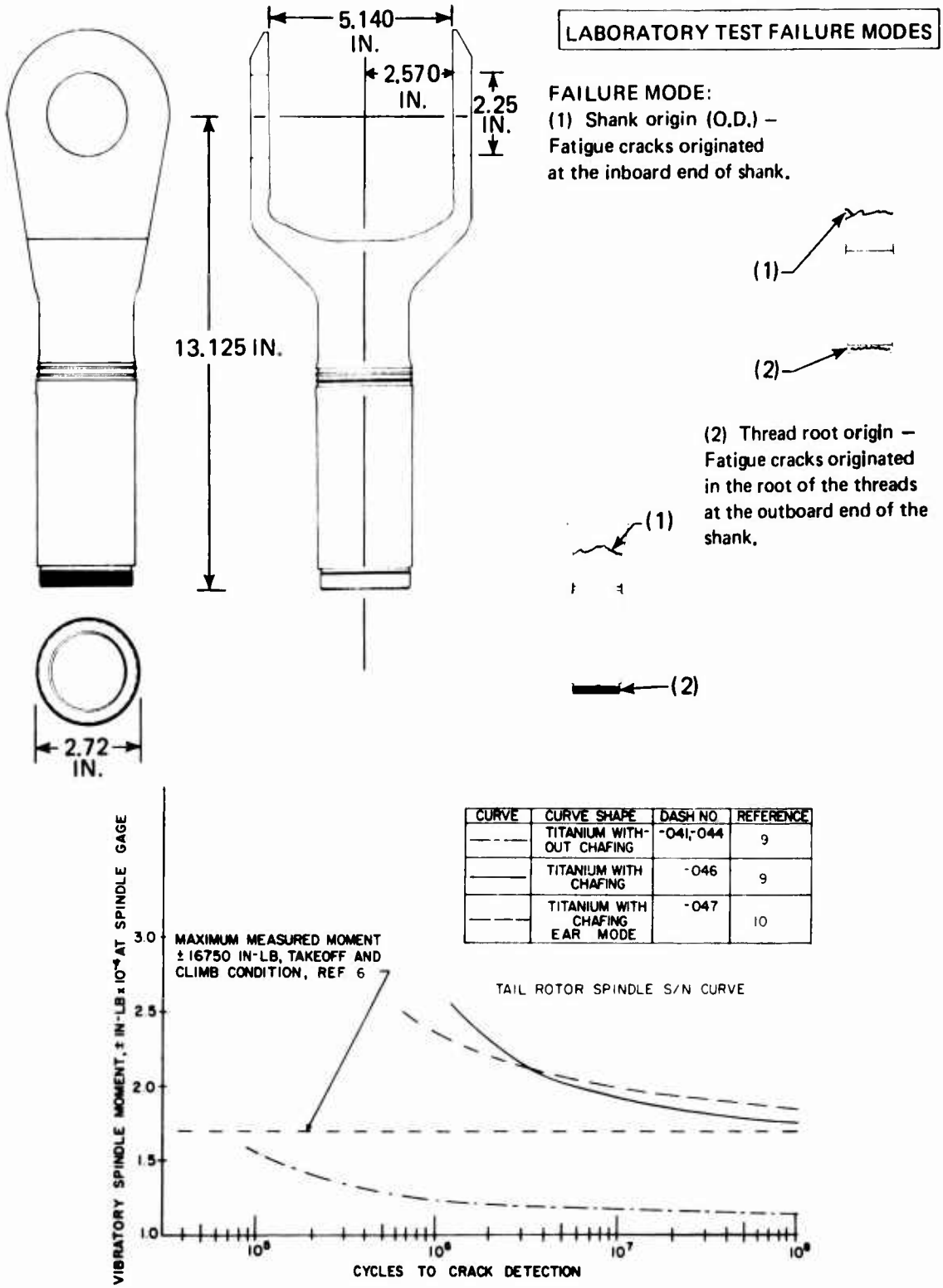

Figure 12. Tail Rotor Spindle Fatigue Substantiation Data.

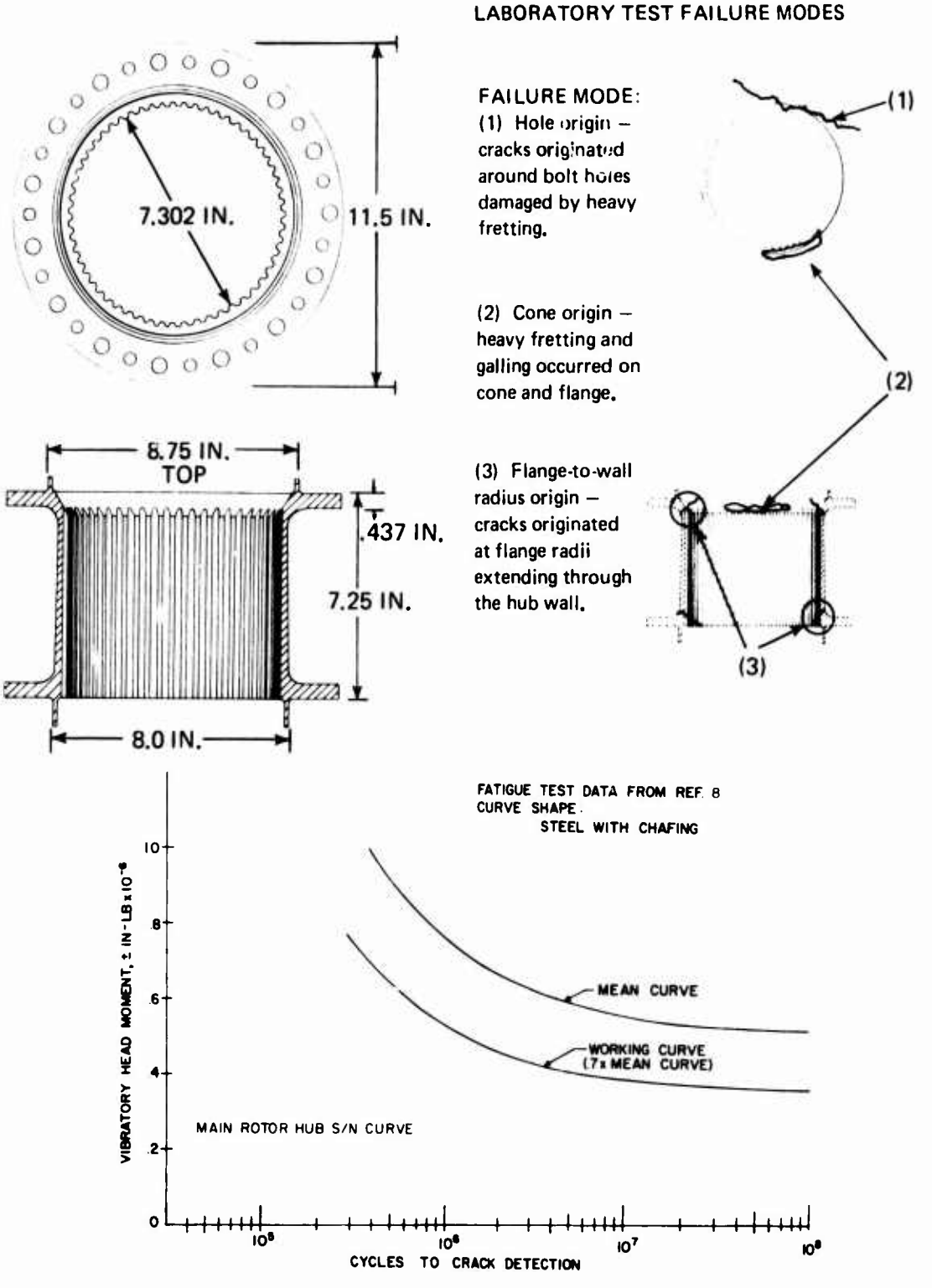

Figure 13. Main Rotor Hub Fatigue Substantiation Data.

TABLE VI. MAIN ROTOR HUB REPLACEMENT TIME CALCULATION

M_H (in.-lb x 10^{-6}) Ref. Table IV	Σ % Time Ref. Table IV	Allowable Cycles x 10^{-6} Ref. Fig. 13	Allowable Hours *	Damage per 100 Hours
.423	1.781	3.8	342	.00520
.438	.1958	3.0	270	.00073
.391	5.508	9.4	846	.00651
.698	.0205	.39	35	.00058
.357	.0280	100.0	9000	0
.395	.00082	8.3	748	0
			Total Damage/100 Hours	.01302

$$\text{Replacement Time} = \frac{100}{.01302} = 7700 \text{ Hours}$$

* Assumes a main rotor speed of 185 rpm and one cycle per revolution.

(e) Magnesium Main Rotor Spacer

The original main rotor spacer was made of magnesium and had an Army replacement time of 4,175 hours. Inspection of in-service parts revealed fatigue cracks initiating at corrosion pits in the central hole of the spacer. As a result, the material for the spacer was changed to aluminum. The two parts have identical dimensions. The magnesium configuration is currently being replaced at overhaul. Since it will be some time before the conversion is completed, an evaluation of the magnesium design was made. The aluminum spacer is analyzed in (f) below.

Mean and working S/N curves for the magnesium main rotor spacer, shown in Figure 14, were taken from Reference 8. Table VII gives the replacement time calculation based upon sample 1 of the operational mission profile.

(f) Aluminum Main Rotor Spacer

Mean and working S/N curves for the aluminum spacer, shown in Figure 15, were taken from Reference 8. Replacement time calculations using the operational mission profile are given in Table VIII. As summarized in Table IX, the aluminum spacer has a replacement time approximately twice that of the magnesium spacer.

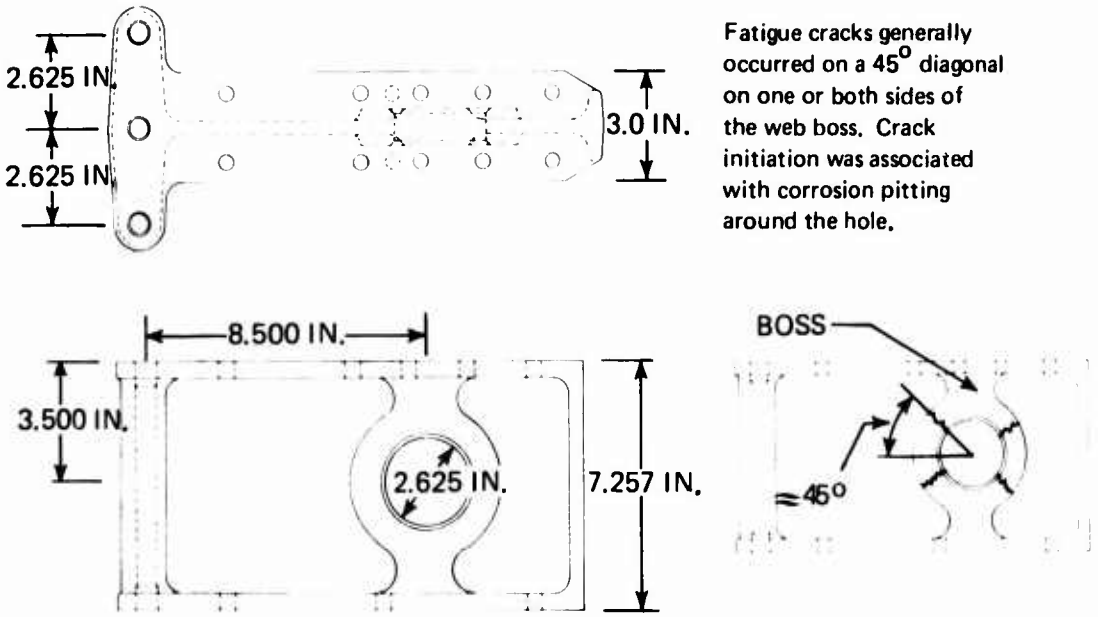

Fatigue cracks generally occurred on a 45° diagonal on one or both sides of the web boss. Crack initiation was associated with corrosion pitting around the hole.

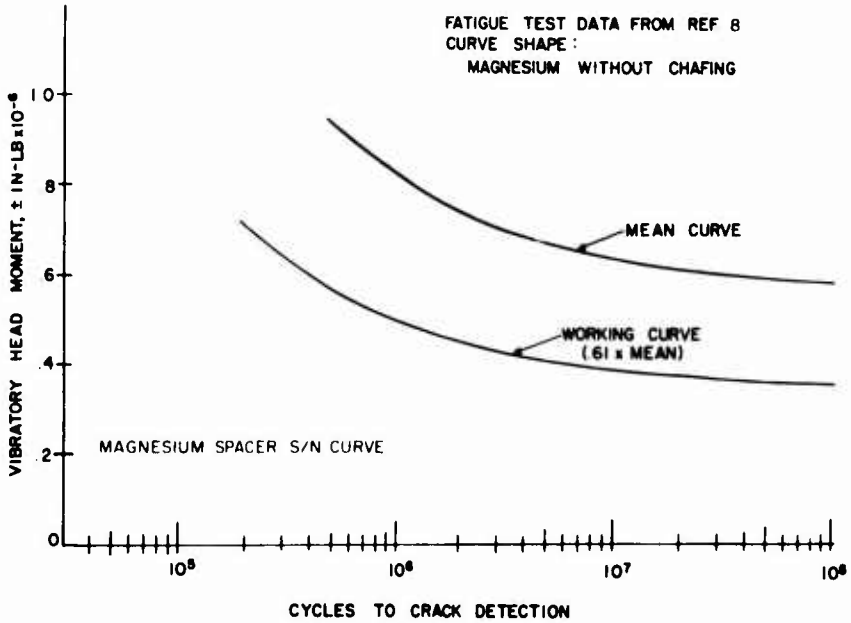

Figure 14. Magnesium Main Rotor Spacer Fatigue Substantiation Data.

TABLE VII. MAGNESIUM MAIN ROTOR SPACER REPLACEMENT TIME CALCULATION

M_H (in.-lb x 10^{-6}) Ref. Table IV	Σ% Time Ref. Table IV	Allowable Cycles x 10^{-6} Ref. Fig. 14	Allowable Hours *	Damage per 100 Hours
.423	1.781	3.3	297	.00599
.438	.1958	2.6	234	.00084
.391	5.508	8.0	720	.00765
.698	.0205	.205	18	.00111
.357	.0280	62.0	5585	0
.395	.00082	7.2	648	0
			Total Damage/100 Hours	.01559

$$\text{Replacement Time} = \frac{100}{.01559} = 6420 \text{ Hours}$$

* Assumes a main rotor speed of 185 rpm and one cycle per revolution.

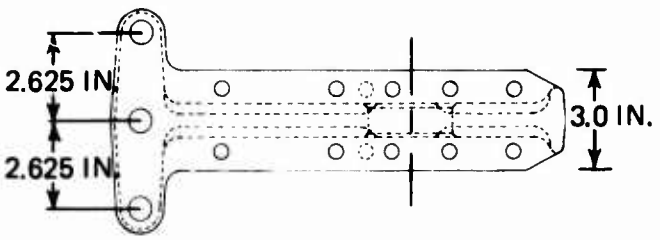

LABORATORY TEST FAILURE MODES

During laboratory fatigue testing, the aluminum main rotor spacer exhibited no fatigue failure.

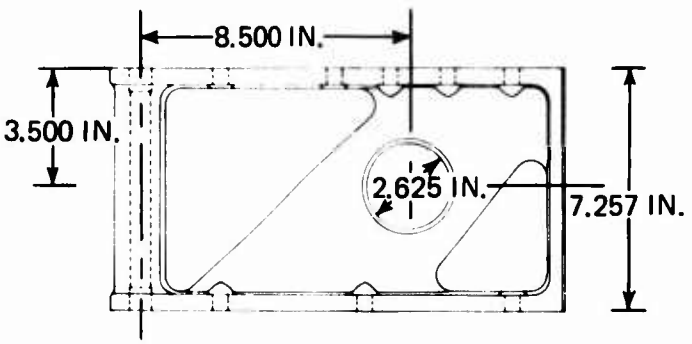

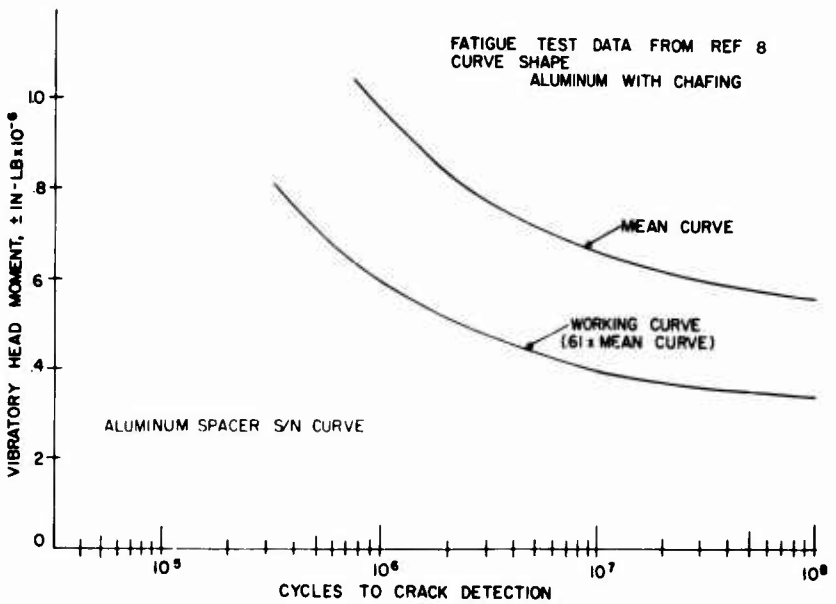

Figure 15. Aluminum Main Rotor Spacer Fatigue Substantiation Data.

TABLE VIII. ALUMINUM MAIN ROTOR SPACER REPLACEMENT TIME CALCULATION

M_H (in.-lb x 10^{-6}) Ref. Table IV	Σ% Time Ref. Table IV	Allowable Cycles x 10^{-6} Ref. Fig. 15	Allowable Cycles *	Damage per 100 Hours
.423	1.781	6.3	568	.00314
.438	.1958	5.1	459	.00043
.391	5.508	12.8	1153	.00478
.698	.0205	.53	48	.00043
.357	.0280	38.0	3423	.00001
.395	.00082	11.8	1063	0
			Total Damage/100 Hours	.00879

Replacement Time = $\frac{100}{.00879}$ = 11380 Hours

* Assumes a main rotor speed of 185 rpm and one cycle per revolution.

TABLE IX. COMPARISON OF COMPONENT REPLACEMENT TIMES

Component	Sikorsky Part No.	U. S. Army Replacement Time	FAA-Approved Replacement Time	Operational Spectrum Replacement Time
Main Rotor Pitch Control Horn	S1510-23350-2	Unlimited	1600	Unlimited
Main Rotor Shaft	6435-20078-014	2500	1300	10400
Tail Rotor Spindle	65112-07002-047	On Condition	2850	Unlimited
Main Rotor Hub	S1510-23001	5275	750	7700
Main Rotor Spacer (Magnesium)	6410-23006-012	4175	750	6420
Main Rotor Spacer (Aluminum)	6410-23016-041	9000 *	9000	11380

* Assumed the same as the FAA-Approved Replacement Time.

CH-54A STRUCTURAL COMPONENT HISTORY

INTRODUCTION

Since the development of the CH-54A, many design improvements have been incorporated into its dynamic component systems. In selecting components for a fatigue study, special attention was given to the main rotor head and tail rotor head assemblies. Six components were analyzed to determine replacement times based on the operational mission profile. Table X describes the parts, their functions in the system, design changes during their service life, and corrective measures taken to prevent problems. Other information includes a summary of part numbers, dash numbers, and aircraft effectivities.

MAIN ROTOR PITCH CONTROL HORN

The CH-54A main rotor pitch control horn (Figure 16), designed and used on the CH-37, functioned as an integral part of the main rotor servos, swashplates, and pushrods. The design never changed during the U.S. Army procurement program except for elimination of blade fold capability. This change saved weight and simplified assembly procedures.

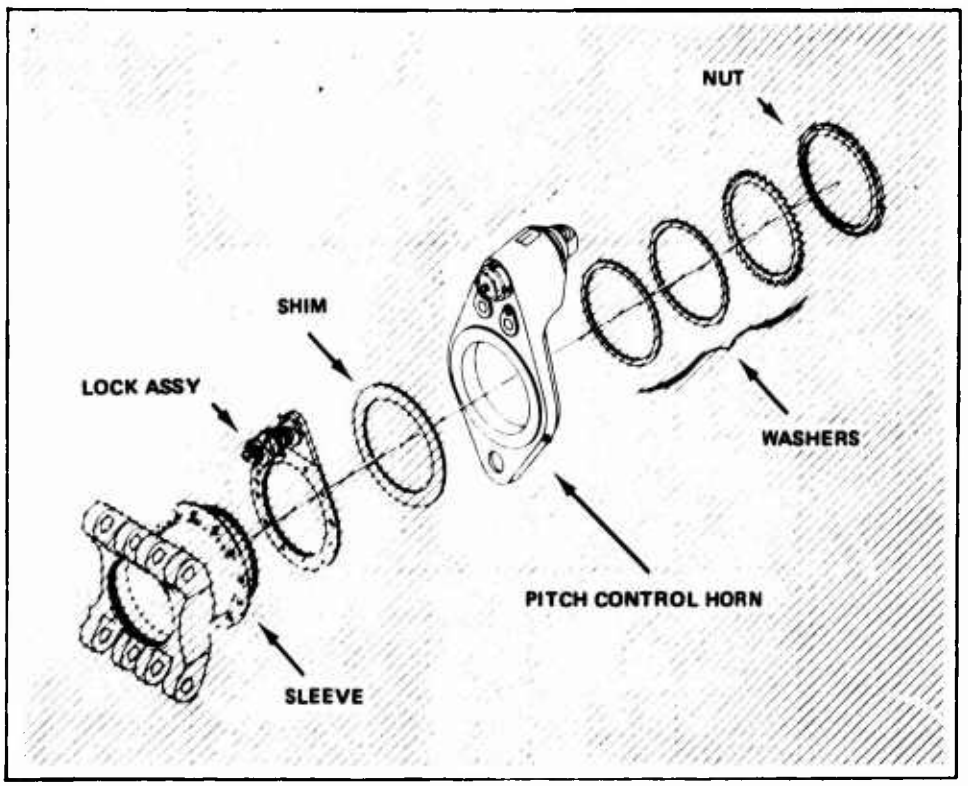

Figure 16. Main Rotor Pitch Control Horn Assembly.

MAIN ROTOR SHAFT

The CH-54A main rotor shaft (Figure 17) was designed to adapt to the new CH-54A main rotor gearbox and to interface with the existing CH-37 main rotor head. The upper end of the shaft was necked down to fit the CH-37 main rotor hub, since the design of the crane helicopter was developed around the CH-37 main rotor system.

Modifications were made in the upper and lower bearing seats during the development stage by incorporating liners to tighten the bearing fit. For the production aircraft, however, wall thicknesses in the bearing seats were increased during manufacturing, thus eliminating the need for the liners. An additional nonstructural improvement was incorporated into the shaft assembly by installing a pressed cork plug in the previously open upper end of main rotor shaft. The plug prevented rain, snow, dirt, and tools from contaminating the interior of the shaft and main gearbox oil sump.

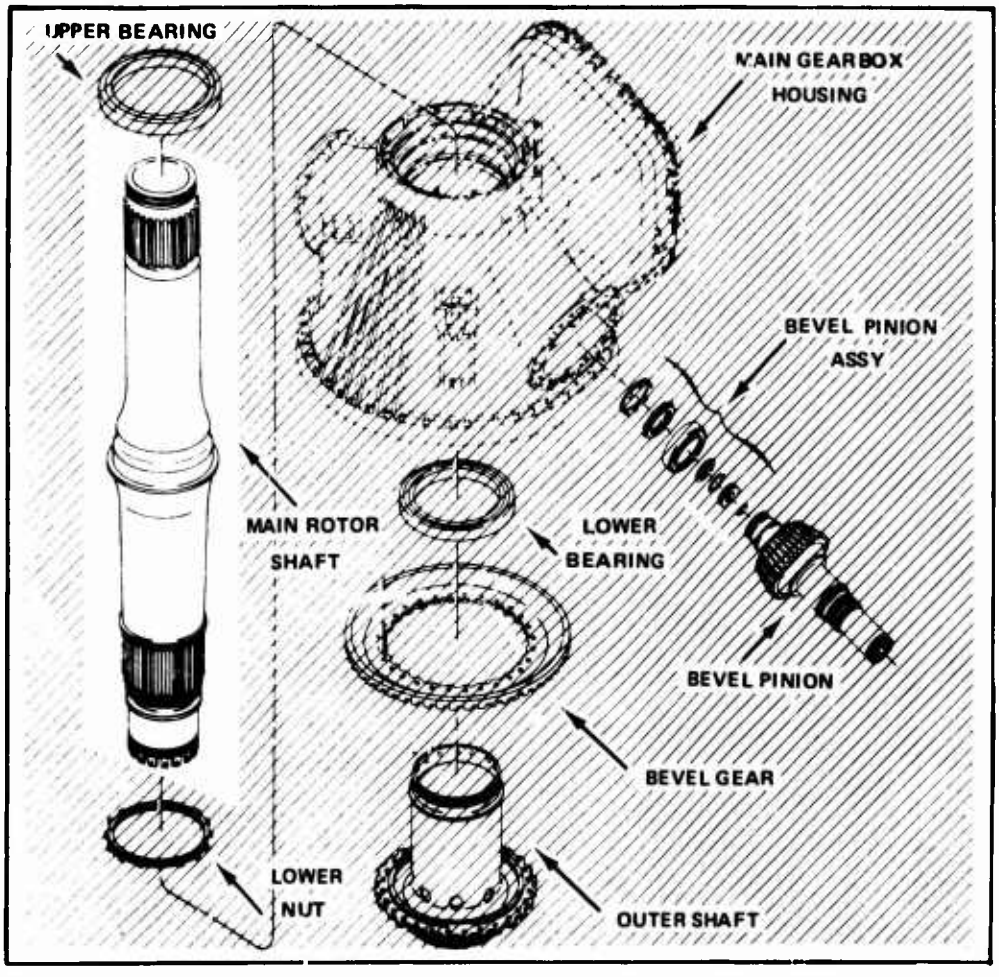

Figure 17. Main Rotor Shaft Assembly.

TAIL ROTOR SPINDLE

As has been stated, the Sikorsky crane was developed with a CH-37 tail rotor system. The first three aircraft were built as a company-funded project, using off-the-shelf tail rotor components, despite certain performance limitations. When the U.S. Army indicated an interest in a crane helicopter, Sikorsky took advantage of the CH-53A program and incorporated its new tail rotor design into the CH-54A. The CH-53A tail rotor provided excellent performance characteristics and appreciable growth potential. That tail rotor was used for the duration of the CH-54A program.

Although fatigue-related structural problems on the tail rotor spindle (Figure 18) were never experienced, design improvements were incorporated to improve fatigue life further (Table X).

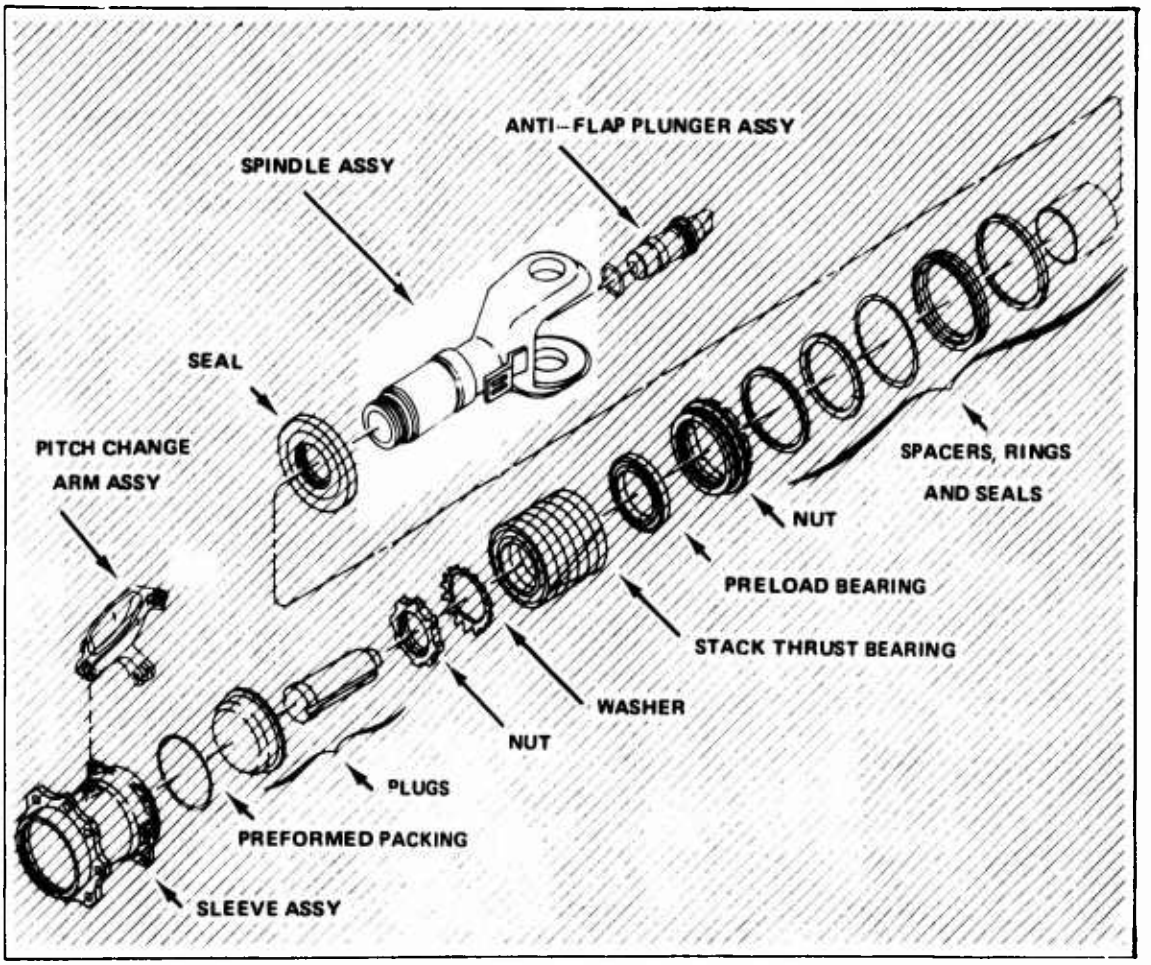

Figure 18. Tail Rotor Spindle Assembly.

MAIN ROTOR HUB

The CH-54A main rotor hub (Figure 19) was designed originally for the CH-37 and later adapted for the crane helicopter as part of the off-the-shelf CH-54A main rotor system. During service on the CH-37, improvements made in the hub increased corrosion resistance and made manufacturing easier. Additional bolt holes were added to the hub flanges during the CH-54A design program to provide added gross weight potential (Table X). No changes in the hub design were ever required to eliminate fatigue damage problems.

MAIN ROTOR HEAD SPACER ASSEMBLY

The main rotor head spacer assemblies (Figure 19) are bolted between each pair of arms of the CH-54A upper and lower main rotor plates. The combination of the upper and lower plates with the six spacers forms an I-beam that reacts vertical bending moments and vertical shear resulting from blade loadings. The spacer itself, acting as a web, reacts shear forces.

Such an assembly was incorporated previously on the five-bladed CH-37. When the same spacer forging was later considered for the CH-54A, lag damper clearance considerations required that a hole be drilled in the spacer web. During whirl stand fatigue testing, cracks developed at the hole, and the spacer had to be redesigned with a boss around the hole. This appeared to solve the problem, but further cracking eventually occurred.

The spacers originally had been machined from magnesium castings. Because magnesium is highly corrosive, the spacers were pitting in normal service environments. High stress concentration around the pit holes caused the magnesium spacers to crack well before their designed replacement time. To solve this problem, the spacer material was changed to aluminum, providing fatigue strength and corrosion resistance superior to those of magnesium.

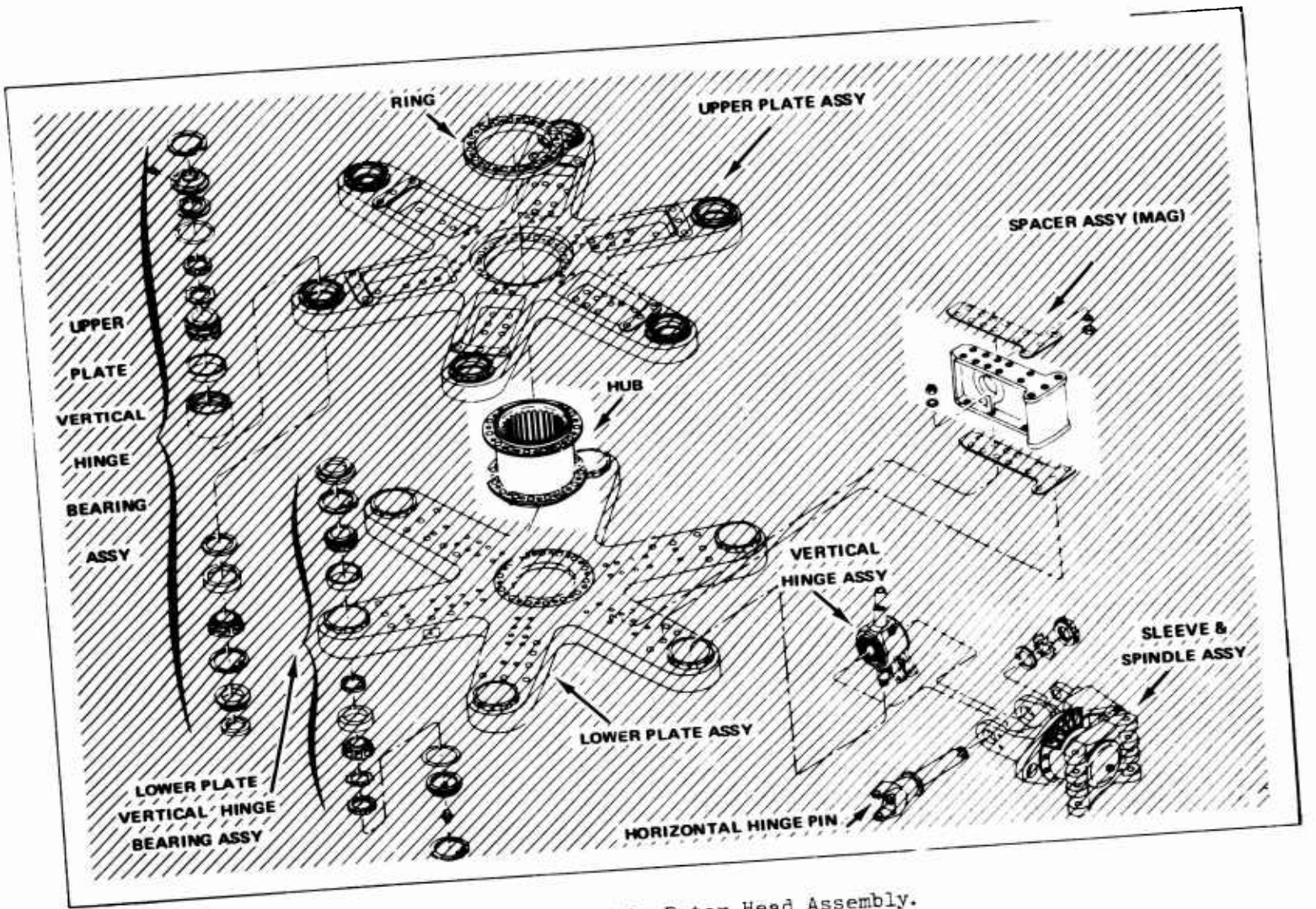

Figure 19. Main Rotor Head Assembly.

TABLE X. COMPONENT HISTORIES

Component	Part Number	Dash No.	Description of Design Change	Reason for Design Change	Remarks
Main Rotor Pitch Control Horn	S1510-23341 of sub-assy. S1510-23350	-1	Original design	-	Used on A/C 64001 thru 64029
	of assy. S1510-23350	-0			
	S1510-23341	-1	Lock pin hole for blade fold omitted - Eliminated manual blade fold capability	No blade fold required on Army aircraft - Elimination of hole reduced chance of incorrect assembly	Used on A/C 64030 and subsequent
	of sub-assy. S1510-23350	-3			
	of assy. S1510-23350	-2			
Main Rotor Shaft Assembly	S6435-20078	-011	Original design	-	Used on A/C 64001 only (-101 shaft)
		-012	Upper bearing seat diameter increased by .0075 in.-Reduced tightness of lower bearing seat liner	Loose upper bearing fit caused fretting of seat - Experimented with lower bearing seat fit	Never used on CH-54A (-101 shaft)
		-013	Same as -012 except reverted to tighter lower liner (same as liner on -011)	-	Never used on CH-54A (-101 shaft)
		-014	Same as -013 except eliminated need for liner by increasing wall thickness	Improved manufacturing of main rotor shaft	Used on A/C 64001, 64004 and subsequent (-104 shaft)
		-015	Same as -014 except added cork seal in shaft opening at upper end	Prevented foreign matter from contaminating gear box oil sump	Incorporated on future spares

TABLE X - Continued

Component	Part Number	Dash No.	Description of Design Change	Reason for Design Change	Remarks
TAIL ROTOR SPINDLE	65112-07002	-041	Original design	-	Used on CH-53A and intended for but never used on CH-54A
		-042	Shank thickness increased, Ear thickness increased-Changed to standard roll threads at end of spindle	Lab tests indicated need for additional strength to accommodate increased loads	
		-043	Same as -042 except ear and spindle shank thickness reduced	CH-53A flight test program revealed loads were lower than anticipated	
		-044	Same as -041 except added extra spacer to assembly	Reverted to original design but added spacer to accommodate dirt exclusion seal	Used on A/C 64001, 64004 through 64009
		-045	Same as -044 except I.D. of spindle reduced and snap ring grooves removed	Design changed to improve fatigue strength	Never used on CH-54A
		-046	Same as -045 except redesigned vernier bracket	Provided more sensitive rigging of tail rotor blade angles	Used on A/C 64010 and subsequent
		-047	Same as -046 except that sacrificial liners added to inside of ears and O.D. of spindle	Increased overhaul interval	Used for retrofit on CH-54A

TABLE X - Concluded

Component	Part Number	Dash No.	Description of Design Change	Reason for Design Change	Remarks
MAIN ROTOR HUB	S1510-23001	-0	Original design (hand forging)	-	These configurations were used on the CH-37 only
		-1	Same as -0 except die forged	Die forging unavailable at start of design - Die forging preferred for structural and fatigue qualities	
		-2	Same as -1 except scallops eliminated from flanges	Easier machining	
		-3	Same as -2 with cadmium plating	Provided corrosion protection	
		-4	Same as -3 except added 15 additional bolt holes in flanges	Increased strength of connection in anticipation of future growth	Used on A/C 64001 and subsequent
MAIN ROTOR SPACER ASSEMBLY	6410-23006	-011	Original design (clearance hole drilled in web)	Hole provided for damper clearance	Used on A/C 64001, 64002 and 64003
		-012	Same as -011 except added boss at clearance hole	Boss provided increased fatigue life	Used on A/C 64004 and subsequent
	6410-23016	-041	Same as 6410-23006-012 except change material to aluminum	Eliminate fatigue cracks around damper clearance hole due to magnesium corrosion	Replacing 6410-23006-012 spacers at overhaul

COMPARISON OF OPERATIONAL AND DESIGN LOADS

INTRODUCTION

TR 70-73 provided a means for comparing peak operational flight loads with static design loads. Except for a few specific peak loads, only approximate peak values could be derived. TR 70-73 reported that most of the recorded data points represented ranges of loads, making it impossible to establish the exact peak value within the range. Table XI compares gross weight, airspeed, main rotor speeds, and maneuver and gust load factors for operational and design conditions. Additional qualifying parameters are included to relate the data effectively.

TABLE XI. COMPARISON OF STATIC DESIGN LOADS WITH OPERATIONAL FLIGHT LOADS

Load Parameter	Operational Flight Loads (Ref. 1)		Static Design
Gross Weight (lb)	44009	a	42000
Airspeed (kn)	120 (KIAS) 132 (TAS) (G.W.= 27000 lb)	a	V_D = 126.5 (TAS) (V_H = 110 (TAS))
Main Rotor Speed (rpm)	198 @ 60 (KIAS) 203 (Hover)	a b	204 (Power on) 215 (Power off)
Load Factor (N_z)	1.88 (Hoist @ 40100 lb) 1.5 (Maneuvers) max. .5 (Maneuvers) min.	a a a	2.26 max. -0.5 min.
Gust Load Factor (N_z)	1.3 max. {25000 lb, 100 (KIAS), 103 (TAS)} 0.6 min. {25000 lb, 100 (KIAS), 103 (TAS)}	a b	1.93 (42000 lb @ 110 TAS)

a Sample No. 1

b Sample No. 2

GROSS WEIGHT AND AIRSPEED COMPARISONS

The CH-54A was designed for a basic gross weight of 42,000 pounds combined with a load factor of 2.26g and a limit dive speed of 126.5 knots. The basic design gross weight also represented the maximum operating weight, since there were no alternate design gross weight provisions for the CH-54A.

TR 70-73 reported that a peak gross weight of 44,009 pounds had been recorded at a speed of 60 knots. Field studies conducted by Sikorsky engineers stationed in Southeast Asia in 1968 indicated that significant numbers of missions were being flown at or above 42,000 pounds. This practice, although possible on the basis of static strength, may have produced damaging loads on fatigue-related components. Overload gross weights probably were flown rarely at speeds higher than 60 to 70 knots or at load factors greater than 1.0 ±0.2g. But even in these low speed and load factor ranges, flapping, power, or control requirements could have approached damaging levels and should have been indicated either by the cruise guide or torque meters. Figure 20 compares load factor vs. gross weight envelopes for design and operational data.

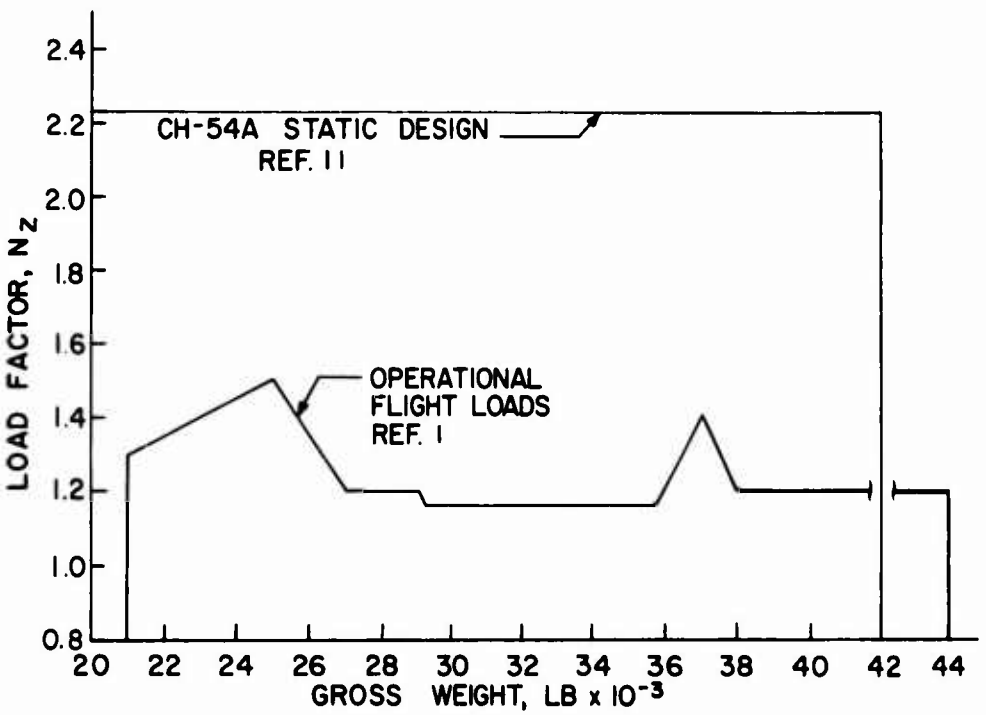

Figure 20. Load Factor Vs. Gross Weight Envelope.

Since more than 30% of the sorties were flown at gross weights in excess of 42,000 pounds, as indicated by Sikorsky field studies, considerations of excessive ride discomfort apparently did not discourage this practice. It is possible that any high cockpit vibration experienced, such as during transition into flare, did not persist long enough to warrant any change in flight practices.

The CH-54A was designed for a limit dive speed (V_D) of 126.5 knots at the design gross weight of 42,000 pounds. The maximum indicated airspeed recorded in TR 70-73 was approximately 120 knots for gross weights of 25,000 and 27,000 pounds. For a density altitude of 5,000 feet, at which this airspeed appeared to be measured, the equivalent true airspeed would be 132 knots. Again, this indicated that structural design limits were exceeded during Southeast Asia operations. In addition to structural limits, a limit operating speed (V_H) of 110 knots was established, because severe nose-down attitudes were experienced at low gross weights for high speeds. Apparently, these redlines were also exceeded (Figure 21).

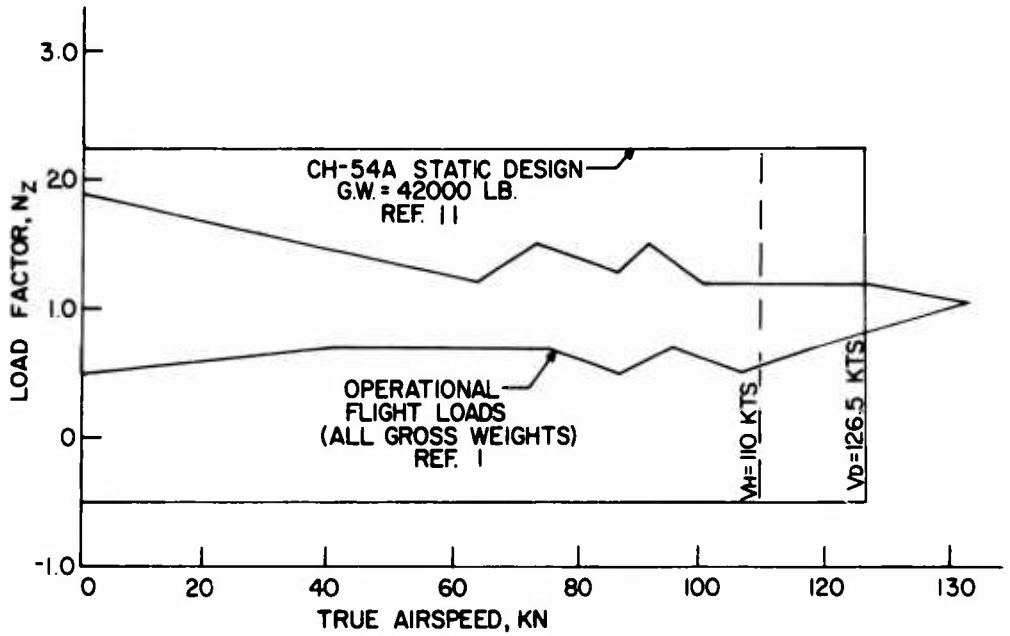

Figure 21. Maneuver V-N_z Diagram.

ROTOR SPEED COMPARISONS

The CH-54A was designed for a main rotor speed of 204 rpm, or 110% N_R (power on), and 215 rpm, or 116% N_R (power off), at 42,000 pounds. The recommended limit operating rotor speed is 194 rpm, or 105% N_R. According to Sikorsky pilots, operation at rotor speeds greater than 105% produces distinct tail rotor whining, well above ordinary noise levels. Pilots normally accept his signal as a warning to cut back rotor rpm.

In Southeast Asia, flight load recorders measured peak main rotor speeds of 198 rpm and 203 rpm, the former occurring in forward flight at 60 knots and 40,344 pounds, and the latter during hover at 25,009 pounds.

These results raised some question. In autorotative flare, it is possible to attain a rotor speed of 198 rpm, but a hover rotor speed of 203 rpm does not sound feasible. This reading indicates either a data recording error or the possibility of poor ground maintenance rigging procedures between the pilot's collective controls and the engines.

MANEUVER AND GUST LOAD FACTOR COMPARISONS

As mentioned above in discussing the CH-54A design gross weight, the design limit load factor (N_Z) is 2.26g. The minimum design load factor as specified in Reference 11 is -0.5g. During the data recording program in Southeast Asia, the cranes operated well within the design load factor limits, as shown in the V-N_Z diagram (Figure 21). Approximately 97% of the peak load factors recorded during maneuvers were experienced at gross weights at or below 29,000 pounds, indicating that no payload was being carried at the time. None of the N_Z occurrences recorded at gross weights greater than or equal to 37,000 pounds exceeded 1.2g in forward flight. The minimum measured load factor was 0.5g in forward flight, well above the design minimum.

Because the basic use of the crane was to pick up and release heavy loads with the single-point winching system, load factor measurements were taken during what was termed the "hoist" mission segment. This type of operation produced a peak N_Z of 1.88g, again below the maximum limit load factor.

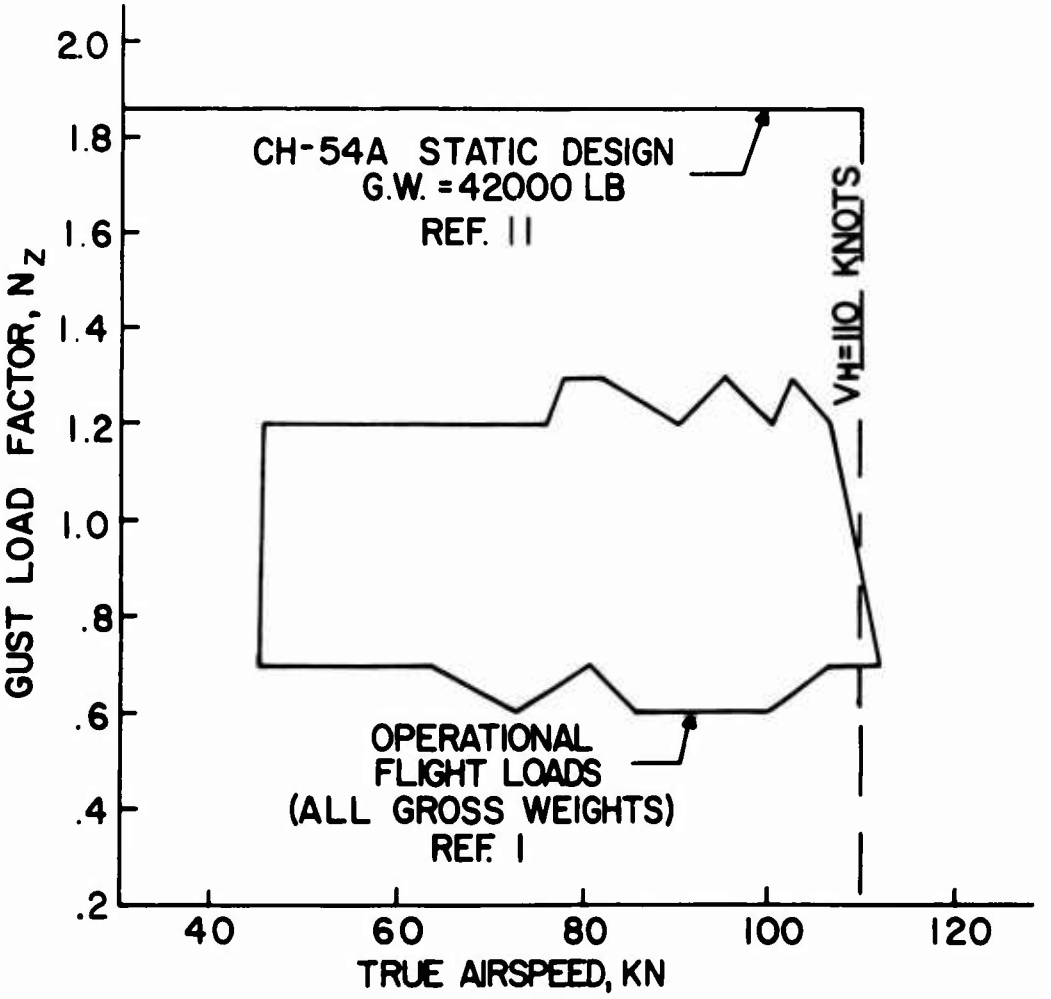

Figure 22. Gust V-N_Z Diagram.

During data editing, gust load factors were distinguished from maneuver and hoist load factors. As indicated by the gust V-N_z diagram (Figure 22), maximum gust peaks were well below the maximum design gust load factor of 1.93g. In addition, the 1.93g design point was applied at a 42,000-pound gross weight and 110 knots, well above the 25,000-pound, 100-knot condition for which a peak gust of 1.3g was measured.

PREDICTION OF LOAD OCCURRENCE FREQUENCY

There are seven helicopter design load parameters for which the frequency of occurrence of peak values must be predicted: maneuver load factor, gust load factor, airspeed, gross weight, rotor speed, horsepower, and main rotor blade flapping. Each parameter is affected by aircraft configuration (weight, drag characteristics, center of gravity, and installed power), payload configuration (drag characteristics, size, single-cable slung loads, or four-point payloads), and aircraft flight profile. These effects govern the magnitude and frequency of occurrence of peak values. Data from TR 70-73 have been employed to establish typical operating limits.

Maneuver Load Factor

Extrapolation of load factor exceedance curves presented in TR 70-73 provides a practical approach for extending the load factor data beyond 200 hours. As a valid sample extrapolation, 5000 hours is selected, in line with 5000-hour replacement times for major dynamic components. Figure 23 indicates that, for a composite load factor spectrum, a peak load factor increment of 1.1g, or a total load factor of 2.1g, would be experienced within 5000 hours.

A similar composite load factor exceedance curve, presented in TR 66-58 (Reference 12), provides similar data. In that study, data were collected during 110.38 hours of military operations in the Fort Benning, Georgia, area. Extrapolation of these data to 5000 hours results in a peak load factor of 1.97.

These two extrapolations of technical report sample data support the assumption that a peak load factor of 2.0g, in combination with the design gross weight configuration, would provide a conservative approach to fatigue design. In addition to extrapolating to 5000 hours, the use of a composite spectrum, which includes all gross weights and the hoist regime load factor occurrences, provides additional conservatism. For airspeeds above 40 knots (IAS), load factor recordings for payload configurations did not exceed 1.4g to 1.5g. The highest load factor recorded was 1.88g, during the hoist regime. However, these hoist load factor pulses are normally of short duration.

A realistic approach to establishing maneuver load factors for fatigue should depend largely on the type of payload. A moderate peak load factor of 1.8g would be employed for configurations involving single-point slung loads. A peak load factor of 2.0g would be applicable to four-point, rigidly attached payloads, such as a pod. When no payload is carried, a

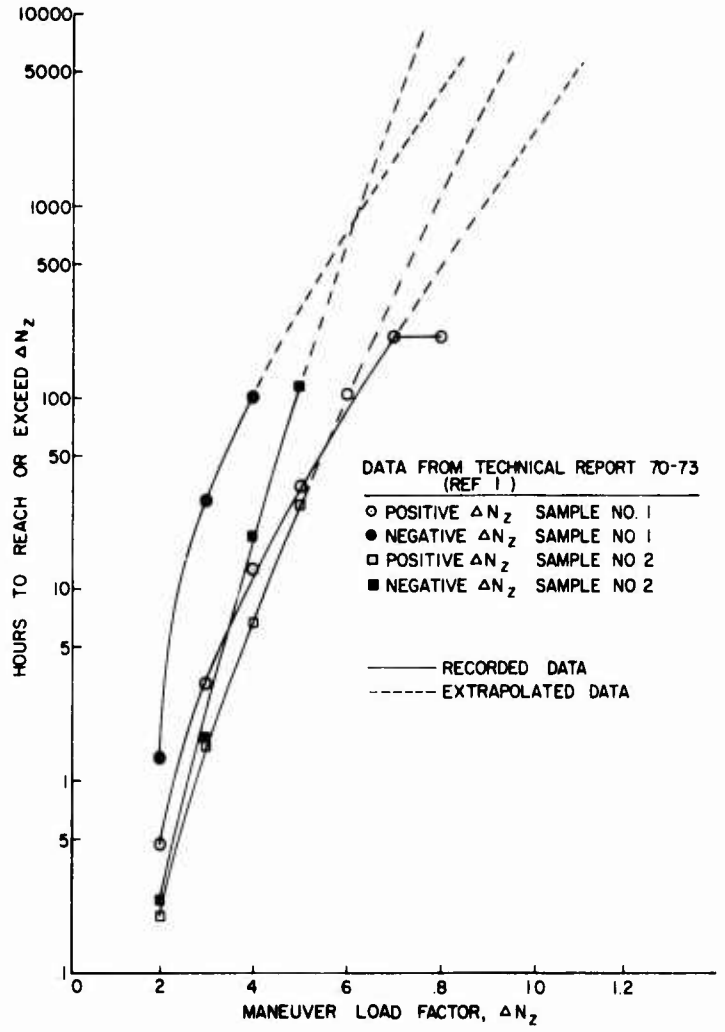

Figure 23. Prediction of Maneuver Load Factors Above 200 Hours.

peak load factor of 2.2g would be applicable. A peak load factor of 2.0g would be employed during pickup and release of payloads.

Gust Load Factor

Gust load factor data from the 200-hour samples of TR 70-73 can be extrapolated validly to 5000 hours. Weather phenomena are assumed to follow a straight-line log-normal distribution. Figure 24 indicates that, for a composite load factor spectrum, a peak gust load factor increment of .44g, or a total load factor of 1.44g, would be experienced within 5000 hours. A similar composite exceedance curve, presented in TR 66-58, provides similar results when extrapolated to 5000 hours. A peak gust load factor of 1.45g is derived from these data. These results suggest that the probability is extremely remote that applied loads from gust response would ever exceed maneuver loa -.

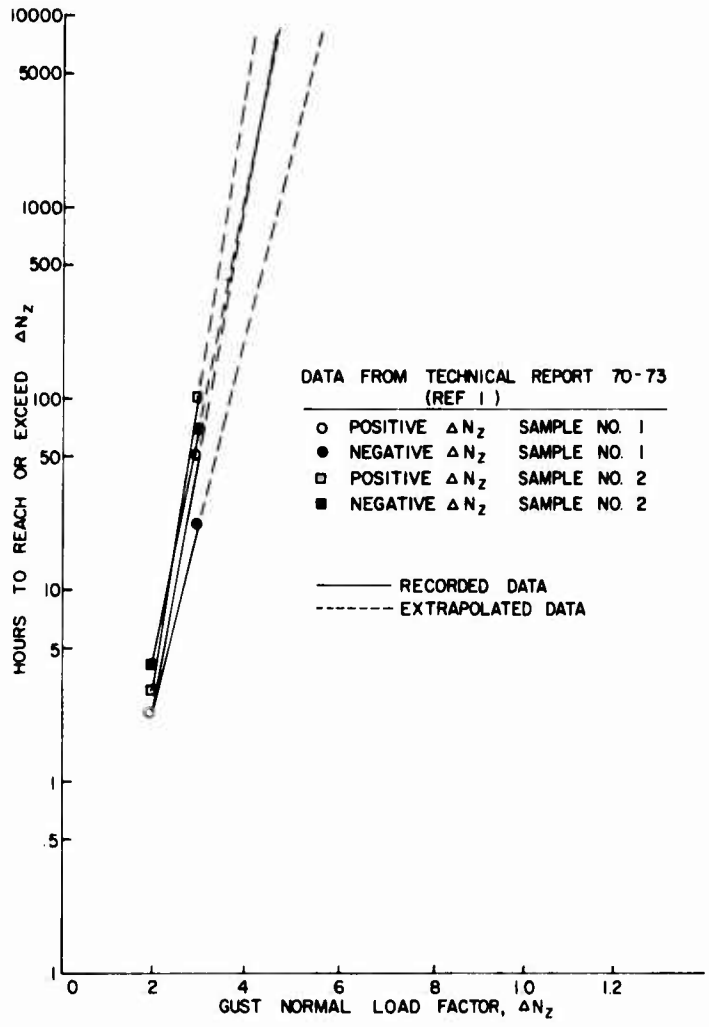

Figure 24. Prediction of Gust Load Factors Above 200 Hours.

Airspeed

Data from TR 70-73 support a realistic airspeed of 100 knots for aircraft configurations involving single-point slung loads. Figures 8 and 9 indicate that 99% of the time in which aircraft gross weights were greater than or equal to 37,000 pounds, airspeeds were 90 knots (TAS) or less. Future crane helicopter fatigue designs should incorporate these facts.

Peak airspeeds for future fatigue designs should realistically depend on the handling quality characteristics of specific externally carried payloads. Payload classes should include a single-point or multipoint carried vehicle, artillery piece, container, or netted cargo, a rigidly attached container or medical pod, and no payload at all.

For example, an approach to development of a speed spectrum for single-point slung loads would be as follows:

a) 99% of the time for slung load configurations is distributed at or below 100 knots. (Figure 9 presents a typical distribution.)

b) The remaining 1% is distributed 75%-25% between 110 knots and 120 knots, respectively.

In considering four-point, rigidly attached loads, handling quality characteristics of the particular payload would be combined with drag and power characteristics to establish a peak airspeed for fatigue analysis. Configurations without payload would be restricted to the limit dive speed established by static design.

Gross Weight

For a fatigue design effort, a three-segment breakdown is sufficient for gross weight distribution. Using the gross weight categories established in the "Operational Mission Profiles" section of this report, the following time distribution was derived from TR 70-73:

Gross Weight	% Time	
	Sample 1	Sample 2
< 29000 lb	60.8	60.4
≧ 29000 lb but < 37000	9.3	10.3
≧ 37000 lb	29.9	29.3

These results provide reasonable support for a 60% - 10% - 30% distribution of time for aircraft weights of 70%, 85%, and 100% of the design gross weight, respectively.

Main Rotor Speed

Since normal variations of main rotor speed are well within the endurance limit of rotor speed related components, 100% rotor speed for 100% of the time is reasonable for development of fatigue spectra. For such components as main rotor and main gearbox bearings, however, for which designs are affected by a rotor speed spectrum, the following distribution is offered, based on data from TR 70-73:

% Rotor Speed	% Time
98-102%	85%
103-106%	14.9%
106-110%	0.1%

Horsepower

There are three essentials for the development of horsepower spectra: mission requirements, engine capability, and rotor performance. Also, rotor performance is dependent on main rotor blade characteristics and aircraft flat plate drag. The variability of these parameters from one aircraft design to another makes prediction of frequency of occurrence inapplicable for horsepower. However, fatigue design capabilities of power-related components often can be assessed quickly by visual inspection of the mission requirements. The extent of hover time, sideward flight time, and high-speed time, coupled with preliminary power data, can aid in establishing peak power requirements in the early stages of fatigue design.

Main Rotor Blade Flapping

A main rotor blade flapping spectrum impacts significantly on the fatigue design of main rotor head dynamic components and main rotor shaft. A peak main rotor blade flapping angle(β) is established, for example, by control limits. A straight-line log-normal distribution of flapping for maneuvers between the peak value and the level flight value is validated by correlation with data from the CH-53A 25-hour flight test substantiation program (Reference 13). This assumes a .0001% probability of occurrence of the peak flapping angle. Level-flight blade flapping values of 3° to 4° are established by Sikorsky flight test.

CONCLUSIONS

1. Hover time during combat operations is approximately one-third to one-half the time currently used for crane helicopter design spectrums.

2. Ascent and descent times during combat operations are approximately four times greater than used for current crane helicopter design spectrums.

3. The level of command from which crane helicopters are currently deployed impacts on normal crane operating gross weight categories. Crane helicopters are rarely employed for missions for which lower gross weight transport helicopters can be substituted.

4. Maximum operating gross weight limits are often deliberately exceeded when it is necessary to transport special items in the Army inventories; for example, trucks, armored vehicles, and artillery pieces.

5. Airspeeds above 90 knots are rarely associated with an external payload configuration.

6. Most aircraft flight time occurs in a density altitude range of 2000 to 5000 feet.

7. In forward flight, load factors rarely exceed 1.3g for external payload configurations.

8. During the hoist regime, load factor peaks are of significant magnitude compared with typical maneuver load factors.

9. Future Army helicopter designs will benefit from improved data collection and editing techniques.

RECOMMENDATIONS

INTRODUCTION

Future Army helicopter designs will benefit from improved data collection and editing techniques. Better definition of discrete ground and flight regimes is required to develop accurate mission profiles. Consideration should be given to development of a composite operational spectrum based upon a combat environment and on peace-time operation. Knowledge of peak loads and specific load parameters, such as main rotor head moment or main and tail rotor flapping angles, would yield more accurate fatigue load prediction.

DATA COLLECTION

Thorough data collection is required to establish discrete flight conditions from the recorded data. The four-segment breakdown (ascent, descent, steady state, maneuver) should be replaced. The current procedure does not provide enough information to derive specific conditions: hover, hover turns, sideward and rearward flight, ascent, descent, etc.

DATA EDITING

The first phase of data editing should begin in the field. Review of raw data after each flight, accompanied by pilot debriefing, would promote accurate correlation of recorded flight loads with specific flight conditions. An effort should be made to define the low-speed range of conditions, such as hover, hover turns, sideward flight, and transitions. Current methods combine data below 40 knots into one category. Assumptions must then be formulated to reduce the data to the desired format.

The method for editing maneuver load factors should be revised to include time during banked turns. The low number of maneuver occurrences reported in TR 70-73 indicates the absence of low-load-factor turns below the 1.2g editing limit.

DATA PRESENTATION

Mission profile analysis would benefit significantly from revised procedures for the grouping and presentation of operational flight loads data. Meaningful combinations of recorded data would be valuable in developing mission profiles and related fatigue spectra.

For example, one specific load parameter, such as rate of climb, should be cross-plotted against time for each important load parameter:

Load Factor (N_z)
Airspeed
Main Rotor Speed
Gross Weight
Altitude
Horsepower

A distribution of each of these parameters could be developed individually as well as collectively, since each would have a common reference. The rate-of-climb parameter helps to establish a general flight regime: ascent, descent, or steady state. A detailed cross-plot with airspeed would establish the precise flight condition within these three flight regimes. Besides load factor exceedance curves, similar plots for airspeed and main rotor speed would be helpful. The airspeed plots would provide a general distribution of airspeeds for cruise and maneuvers, and the rotor speed plots would provide valuable information for rotor and gearbox bearing design. Information on load attachment methods would be helpful, whether single-cable slung loads, hard-point connections, shade roller connections, or no payload.

The availability of specific operational hardware load parameters would prove beneficial in establishing operational trends. Valuable information would be gained for future main and tail rotor fatigue designs if data were available for main rotor blade flapping, tail rotor flapping, tail rotor collective, and tail rotor thrust. Ideally, these data would be presented along with rate of climb and airspeed.

FUTURE STUDIES

An operational mission profile, such as that developed from TR 70-73, does not provide an absolute design tool. Certain limiting conditions, which were prevalent during Southeast Asia operations, affected the results. For example, hover time was not typical for universal crane operations. The level of command from which aircraft were deployed restricted gross weight operating ranges. The evasive flight tactics adopted for combat operation may have impacted on flight procedures.

Additional analytical studies are recommended to examine the need for a weighted composite design spectrum that would encompass the full use of the CH-54A in U. S. Army military operations. It would add accuracy and realism to future crane helicopter designs.

LITERATURE CITED

1. Giessler, F. Joseph, et al., FLIGHT LOADS INVESTIGATION OF CH-54A HELICOPTERS OPERATING IN SOUTHEAST ASIA, Technology Incorporated; USAAVLABS Technical Report 70-73, Eustis Directorate, U. S. Army Air Mobility Research and Development Laboratory, Fort Eustis, Virginia, January 1971, AD 881238.

2. Naval Air Systems Command, STRUCTURAL DESIGN REQUIREMENTS (HELICOPTERS), Department of the Navy; AR-56, February 17, 1970.

3. Sikorsky Aircraft, FLIGHT TESTS FOR STRUCTURAL SUBSTANTIATION OF THE S-64 HELICOPTER INCLUDING PERFORMANCE AND VIBRATION MEASUREMENTS, SER-64095, April 9, 1964.

4. Sikorsky Aircraft, ADDITIONAL FLIGHT TESTS FOR FAA CERTIFICATION OF THE S-64A HELICOPTER, SER-64137, April 15, 1964.

5. Sikorsky Aircraft, STRUCTURAL SUBSTANTIATION OF THE S-64E MAIN ROTOR HEAD AND CONTROL SYSTEM FOR FAA CERTIFICATION, SER-64470, May 7, 1969.

6. Sikorsky Aircraft, EXTENSION OF FAA V_{ne} CERTIFICATION OF THE S-64E, SER-64471, May 19, 1969.

7. Sikorsky Aircraft, FATIGUE SUBSTANTIATION OF THE YCH-54A/S-64E MAIN ROTOR HEAD CONTROL COMPONENTS BASED ON LABORATORY AND FLIGHT TEST DATA, SER-64104, March 12, 1965.

8. Sikorsky Aircraft, S-64 MAIN ROTOR WHIRL/FATIGUE TEST RESULTS, SER-64564, July 6, 1971.

9. Sikorsky Aircraft, FATIGUE SUBSTANTIATION C S-64A/S-64E AUXILIARY ROTOR ASSEMBLY, SER-64103, March 29, 1965.

10. Sikorsky Aircraft, FATIGUE SUBSTANTIATION OF CH-53A ROTARY RUDDER OUTPUT SHAFT, HUB, AND BLADE RETENTION COMPONENTS, Test Report, SER-65076, November 26, 1965.

11. Sikorsky Aircraft, STRUCTURAL DESIGN CRITERIA REPORT - MODEL S-64A HELICOPTER, SER-64091-1, May 16, 1966.

12. Braun, Joseph F., and Giessler, F. Joseph, CH-54A SKYCRANE HELICOPTER FLIGHT LOADS INVESTIGATION PROGRAM, Technology Incorporated; USAAVLABS Technical Report 66-58, U. S. Army Aviation Materiel Laboratory, Fort Eustis, Virginia, June 1966, AD 638364.

13. Sikorsky Aircraft, AIRCRAFT MISSION SIMULATION AND FLIGHT LOAD MEASUREMENT PROGRAM, Test Report, SER-65417, May 24, 1968.